University of Central Florida

RAGHAVAN RESEARCH GROUP

UTSR University Turbine Systems Research

In-situ Optical Monitoring of Operating Gas Turbine Blade Coatings Under Extreme Environments

2020 Sensors and Controls Project Review Meeting

Quentin Fouliard, Post-doctoral Fellow

Co-PI: Ranajay Ghosh

PI: Seetha Raghavan

https://aerostructures.cecs.ucf.edu/

Aug 26, 2020

Overall goals

- Develop and demonstrate at the laboratory scale an advanced optical suite of instrumentation technologies for enhanced monitoring of gas turbine thermal barrier coatings (TBCs).

- Specific goals are to improve the accuracy and effectiveness of temperature and strain measurements made on high temperature gas turbine blades.

Project Objectives

- Achieve intelligent sensing that leverages intrinsic properties of coatings and dopants through optical emission and absorption characteristics while ensuring coating integrity and durability goals are concurrently met.

- Achieve accurate diagnostics of turbine blade coatings under operating environments.

- Achieve advances in benchmarked optical measurement technologies in existing laboratory replicated environments.

Project Tasks

Task 1: Project Management & Planning
Task 2: Define and manufacture sensor configuration
Task 3: Establish Sensing Properties and Characterize Coating Response for Luminescence Based Sensor
Task 4: Perform Non-Intrusive Benchmarking Measurements of Surface Temperature and Strain
Task 5: Develop and Test Laboratory Scale Sensor Instrumentation Package

Overview of project advancement and results

- **Background, Motivations & Objectives**
  - Thermal Barrier Coatings and their benefits
  - Need for **higher accuracy of temperature measurements**
  - Need for **improved method for coating damage monitoring**

- **Phosphor Thermometry experimentation**
  - Phosphor Thermometry system setup
  - Decay and intensity results on an innovative co-doped YSZ:Er,Eu coating
  - Modeling results and measurements in the presence of a thermal gradient

- **Coating damage monitoring**
  - Coating delamination monitoring concept
  - Modeling results
  - Experimental results
  - Luminescence trade-offs and coating optimization

- **Conclusions and perspectives**

Background, Motivations & Objectives

Thermal Barrier Coatings (TBCs)

- **Thermal barrier coatings (TBCs)** used in combination with air cooling to protect metal substrates from extreme temperatures in the high-pressure turbine (1300 - 1600°C)

Clarke, D (2012). *MRS Bulletin*, 37(10), 891-898

  - Air film cooling: ΔT= -100 to -400°C

Kotowicz, J, et al. *Archives of Thermodynamics* 37.4 (2016): 19-35

  - **TBC: ΔT= -150 to -200°C [3,4,5,6]**

Sobhanverdi, R. and Alireza A. *Ceramics International* 41.10 (2015): 14517-14528.
Bacos, M. P., et al. *Review of ONERA Activities* (2011).
Darolia, R. *International Materials Reviews* 58.6 (2013): 315-348.
Xu, Li, et al. *Procedia Engineering* 99 (2015): 1482-1491.

- **Major applications:**
  - Aeroengines
  - Power generation engines

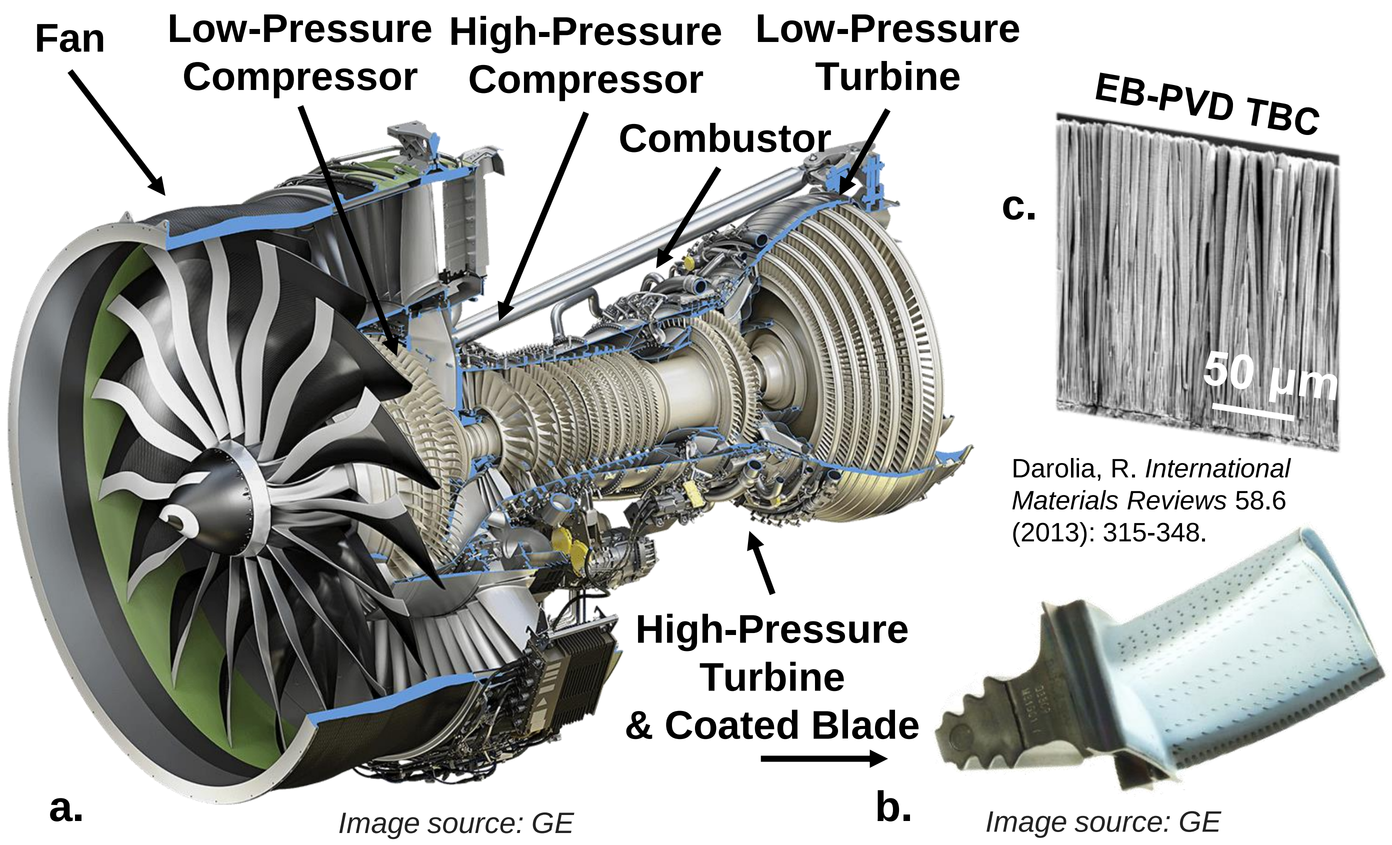

a) Cutaway view of the new GE9X aircraft engine
b) Photograph of a turbine blade coated with TBC
c) SEM micrograph of an EB-PVD TBC top coat

Review of TBC materials properties

TBC layer Typical composition	**Top coat** **7-8wt.%YSZ**	**TGO** $\mathbf{Al_2O_3}$	**Bond coat** **NiCrAlY / PtAl**
Thermal conductivity λ at 1100°C (W/(m·K))	**1-3** [1,2,4,5]	**5-6** [4,6]	**34** [5]
Coefficient of thermal expansion α ($\times 10^{-6}$ K^{-1})	**11-13** [3,4,7,8]	**7-10** [3,7,8,9]	**13-16** [3,7,8,9]
Elastic modulus (GPa)	**0-100** [13]	**320-434** [3,7,8,9]	**110-240** [3,7,9]
Toughness K (MPa· √m)	**0.7-2.2** [7,10]	**2.8-3.2** [7,11]	**>20** [7]
Poisson's ratio ν	**0.2** [8]	**0.2-0.25** [8,9]	**0.3-0.33** [8,9]
Oxygen diffusivity at 1000°C (m^2/s)	$\mathbf{10^{-11}}$ [4]	$\mathbf{10^{-19}}$**-**$\mathbf{10^{-21}}$ [4,6]	-
Crystal microstructure (phase) Stable up to	t' **1200°C** [12]	α **1750°C**	β, γ **1050°C**

[14]

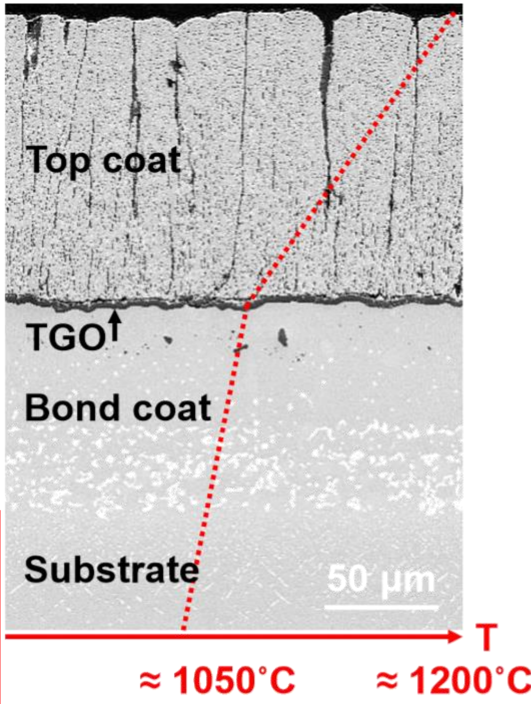

[1] Dinwiddie, Ralph B., et al. No. CONF-9606158-1. Oak Ridge National Lab., TN, USA, 1996
[2] Nicholls, John R., et al. *Surface and Coatings Technology* 151 (2002): 383-391.
[3] Liu, Jing., *PhD dissertation University of Central Florida* (2007).
[4] Lee, Woo Y., et al. *Journal of the American Ceramic Society* 79.12 (1996): 3003-3012.
[5] Lim, Geunsik, and Aravinda Kar. *Journal of Physics D: Applied Physics* 42.15 (2009): 155412.
[6] Steenbakker, Remy. *PhD dissertation Cranfield University*, (2008).
[7] Rabiei, et al. *Acta materialia* 48.15 (2000): 3963-3976.
[8] Yang, Lixia, et al. *Surface and Coatings Technology* 251 (2014): 98-105.
[9] Busso, E., et al. *Acta materialia* 55.5 (2007): 1491-1503.
[10] Liu, Y. et al. *Surface and Coatings Technology* 313 (2017): 417-424.
[11] Petit, J. *PhD dissertation University Pierre été Marie Curie – Paris VI* (2006).
[12] Witz, G., et al. *Advanced Ceramic Coatings and Interfaces II: Ceramic and Engineering Science Proceedings, Volume 28, Issue 3* (2007): 39-51.
[13] Renusch, D., et al. *Materials and corrosion* 59.7 (2008): 547-555.
[14] Fouliard, Q. *PhD dissertation University of Central Florida* (2019).

UCF

TGO formation in TBCs

Importance of controlling the operating temperature

- **Logarithmic growth limited by the low oxygen diffusivity through the TGO:**

$$3\beta NiAl + \frac{3}{2}O_2 \rightarrow \gamma' Ni_3Al + \alpha Al_2O_3$$

Liu, Y. Z., et al. *Journal of the European Ceramic Society* 36.7 (2016): 1765-1774.
Bernard, B., *PhD dissertation, Université de Lorraine* (2016)

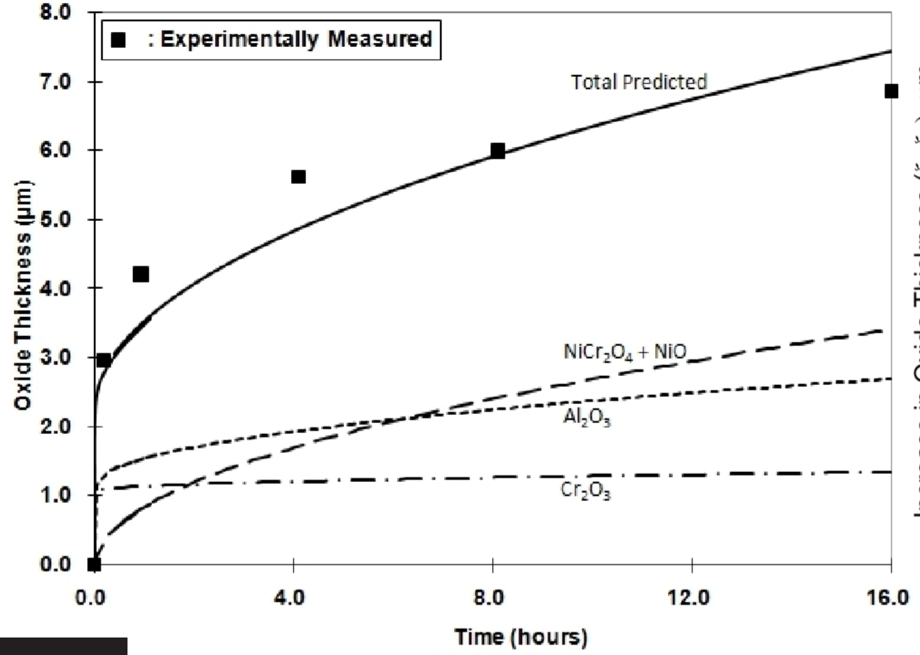

Wu, B, et al. *Journal of the American Ceramic Society* 72.2 (1989): 212-218.

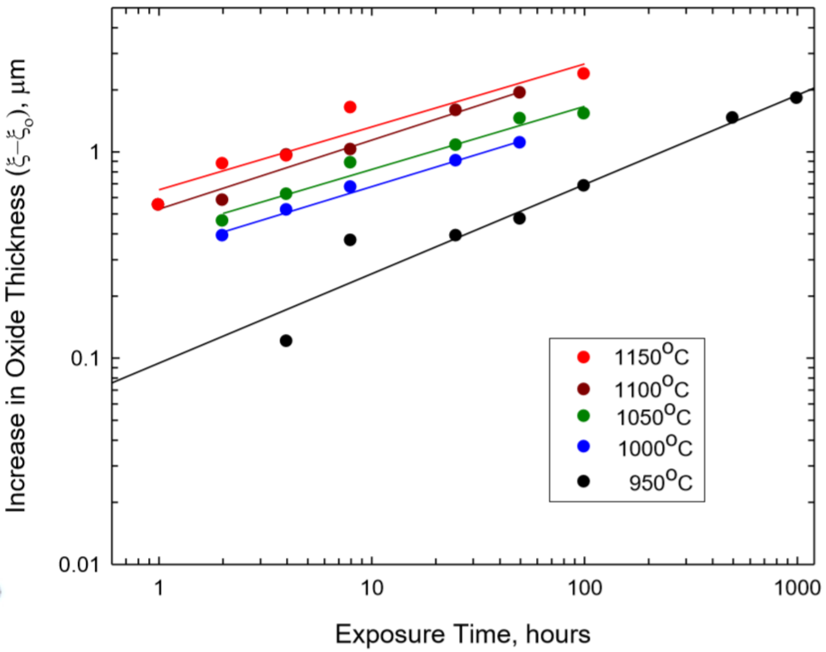

Jackson, R, *PhD dissertation University of Birmingham* (2009)

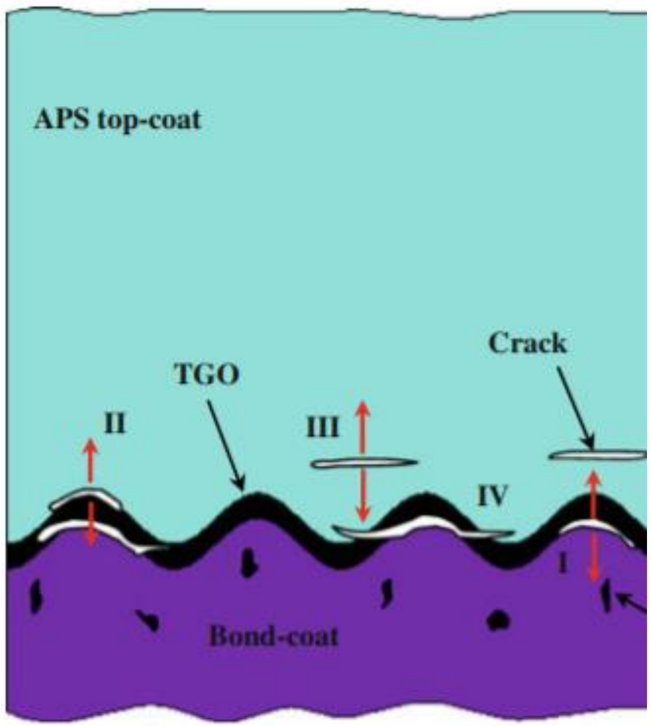

Wang, L., et al *Journal of thermal spray technology* 23.3 (2014): 431-446.

Temperature drives oxide growth in TBCs and is a key factor in coating failure

Phase stability in Thermal Barrier Coatings (TBCs)

Importance of controlling the operating temperature

- **Standard top coat material**: 7-8wt.% (4-4.5 mol.%) YSZ optimal for resistance to spallation and thermal stability Patnaik, P. et al, National Research Council Of Canada Ottawa, Ontario (2006)
  - **Y^{3+} introduces oxygen vacancies that stabilizes t'**

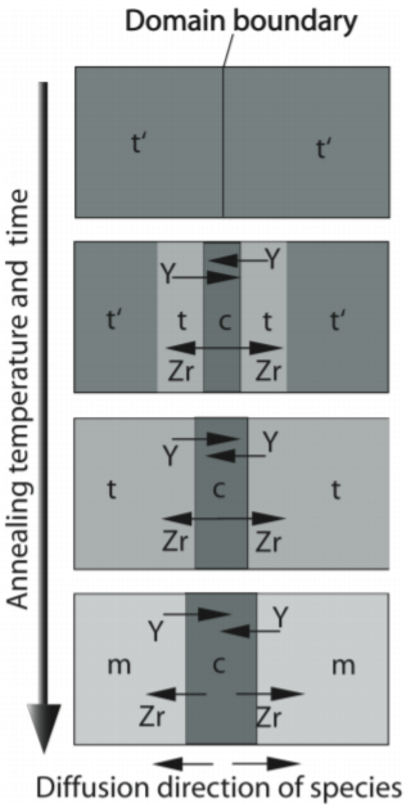

Witz, G., et al. *Advanced Ceramic Coatings and Interfaces II: Ceramic and Engineering Science Proceedings, Volume 28, Issue 3* (2007): 39-51.

- **High temperature sintering of t'-YSZ:**
  - **Pore coarsening → thermal conductivity increase** Guignard, A. *Vol. 141. Forschungszentrum*, Jülich, (2012).
  - **Crack forming**
- **t' phase stable up to 1200°C:**
- $$t' \xrightarrow[1200°C]{} t + c \xrightarrow[600°C]{} m + c$$ $\Delta V = +4\%$

Accurate control of TBC operating temperature is needed to control degradation of coatings.

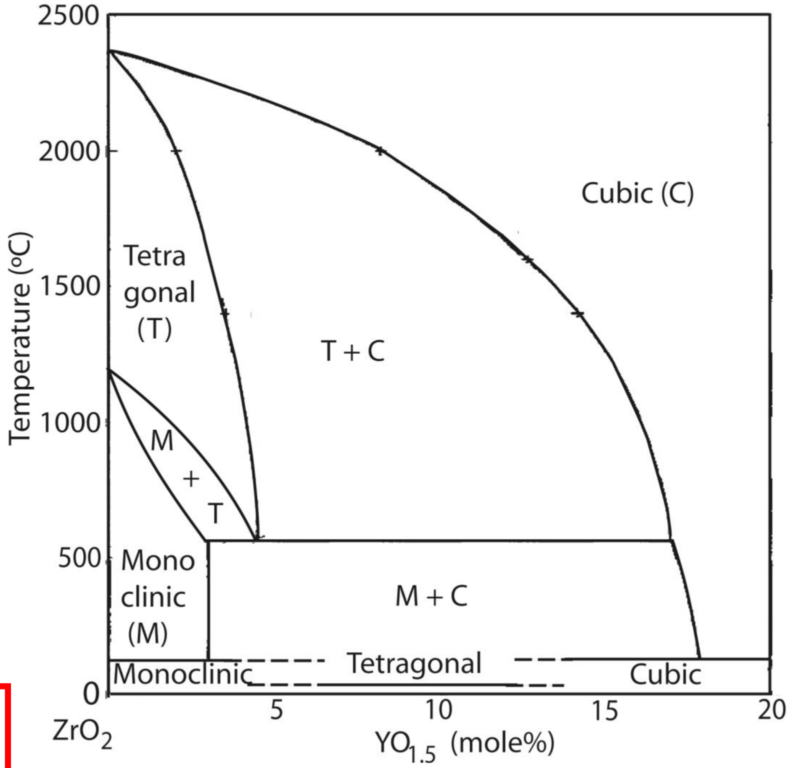

Witz, G., et al. *Advanced Ceramic Coatings and Interfaces II: Ceramic and Engineering Science Proceedings, Volume 28, Issue 3* (2007): 39-51.

Significance of TBC temperature measurements

- State-of-the-art TBCs are not being used to their highest potential because of uncertainties in temperature measurements at high-temperature.
  - Safety margins as high as 200°C are used.

Steenbakker, R, (2009) *Journal of Engineering for Gas Turbine and Power*, 131-4 p 041301

- Ideal Brayton cycle efficiency: $\boldsymbol{\eta = 1 - \frac{T_c}{T_t}}$

η: cycle efficiency, $\frac{T_c}{T_t}$: temperature ratio compressor exit / turbine inlet.

- 1% efficiency improvement can save $20m in fuel over the combined-cycle plant life.

- A 130°C increase leads to a 4% increase in engine efficiency.

Ruud, J, (2003). *Performance of the Third*, 50 pp 950-4.

- Failure mechanisms are driven by temperature conditions in the depth of the TBC.

Problem statement:

Accurate determination of thermal gradients in Thermal Barrier Coatings (TBCs) is critical for the safe and efficient operation of gas turbine engines.
Failure mechanisms are thermally activated during engine operation, uncertainty in temperature measurements contribute significantly to lifetime uncertainty.

Measurement techniques for *in-situ* temperature evaluation of TBCs

	Thermocouples	Infrared Thermometry	Phosphor Thermometry
Temperature range (˚C)	-250 – 2320	-50 – 2000	-250 – 1700
Advantages	- Inexpensive - Wide temperature range	- Wide temperature range - Non contact method - Fast response time	- **Non contact method** - **High sensitivity at high temperatures** - **Fast response time** - **Usable on rotating parts** - **Low sensitivity to turbine environment (aging and contamination)**
Drawbacks	- Intrusive probe - Disrupts flow patterns - Not chemically stable in all environments - Low accuracy - Unusable on rotating surfaces	- Optical access required - Sensitive to stray light (flames) - Sensitive to emissivity variations	- Optical access required - Signal weakening at high temperatures

Gas turbine efficiency

Components lifetime

Other critical failure mechanisms: Foreign object damage / Erosion

Importance of controlling coating health

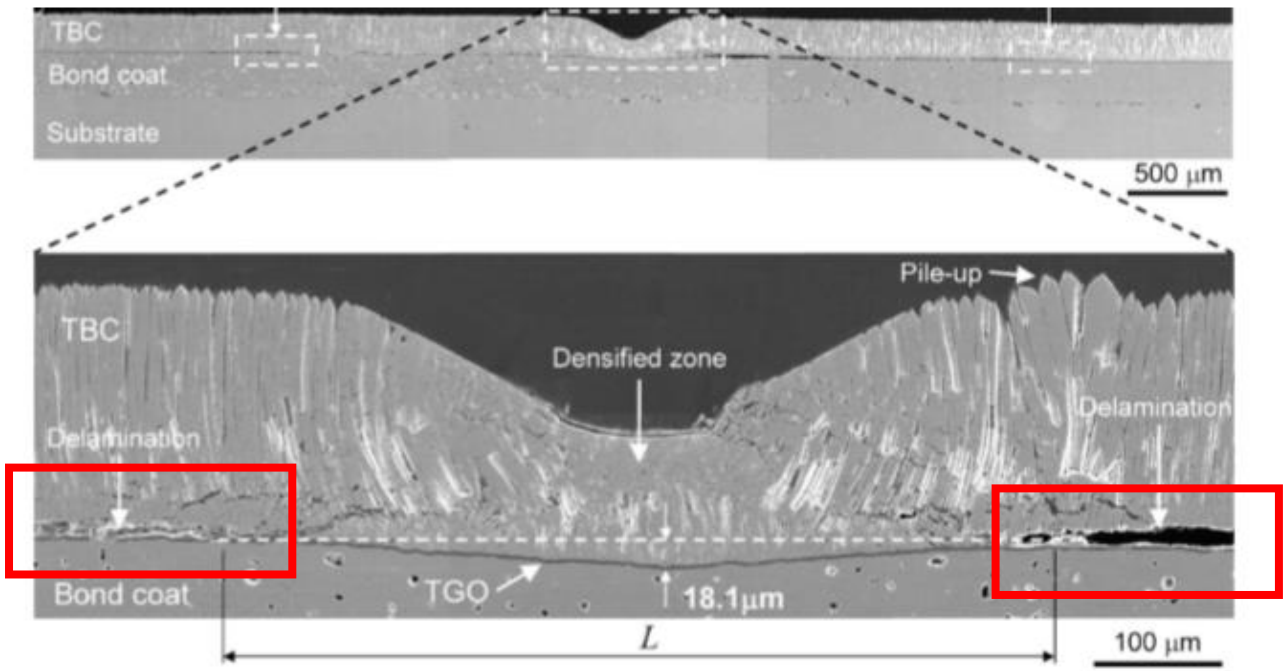

Tanaka, Makoto, Yu-Fu Liu, and Yutaka Kagawa. *Journal of Materials Research* 24.12 (2009): 3533-3542.

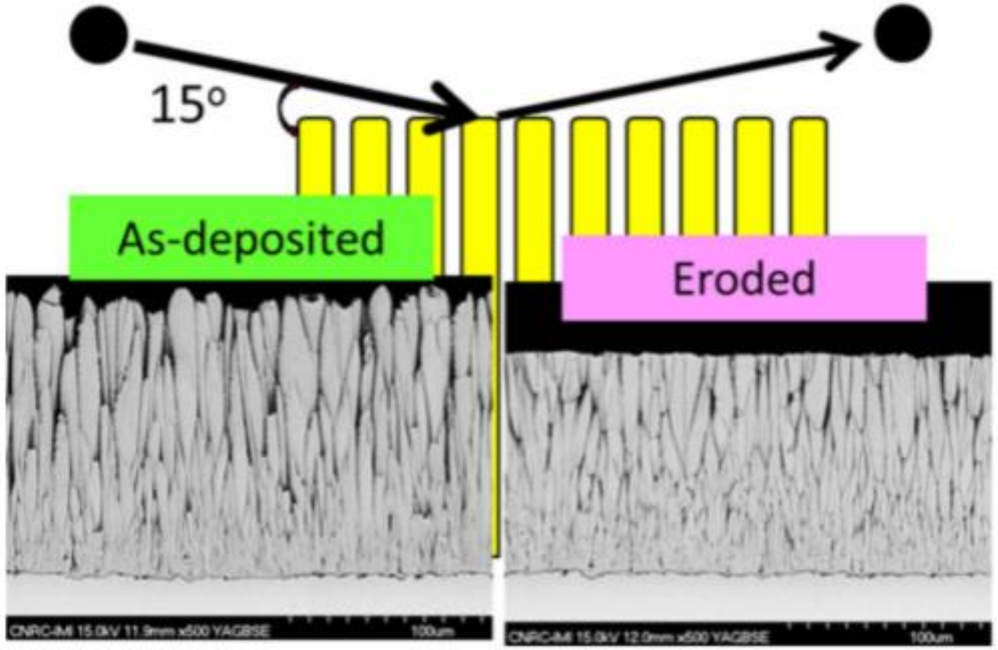

Lima, Rogerio S., Bruno MH Guerreiro, and Maniya Aghasibeig. *Journal of Thermal Spray Technology* 28.1-2 (2019): 223-232.

- Unpredictability of the impact damage/erosion
- Amount of degradation

→ **Importance of improving methods for detection and quantification of delamination**

Direct damage monitoring methods

- Thermal/optical imaging techniques;

  - Infrared thermography in mid-wave or long-wave infrared, post-exposition to an intense heat source (generally a flash of light).
  - Tomography
  - Laser scattering
  - Luminescence-based mapping (in-situ or ex-situ monitoring), under excitation at specific wavelength.

Luminescence imaging provides:

- **Finer spatial resolution**
- **Richer information through spectral features**

Proposed solutions & key objectives

- **Better temperature control in gas turbine engines is needed to improve efficiency and reduce maintenance costs**

→ Implementation of phosphor thermometry instrumentation with accuracy/precision improvement vs. current state-of-the-art

→ Determination of precise sub-surface location of phosphor thermometry measurement point

- **Intense operation of TBC systems result in coating failure that impacts engine availability**

→ Development of a novel approach for delamination monitoring using luminescent coatings (compatible with phosphor thermometry coatings)

Phosphor Thermometry measurements

Part of tasks 2, 3, 4 & 5

Background - Phosphor Thermometry – luminescence decay method

- The time dependent intensity is measured following the excitation pulse to determine the temperature dependent decay time $\tau(T)$.

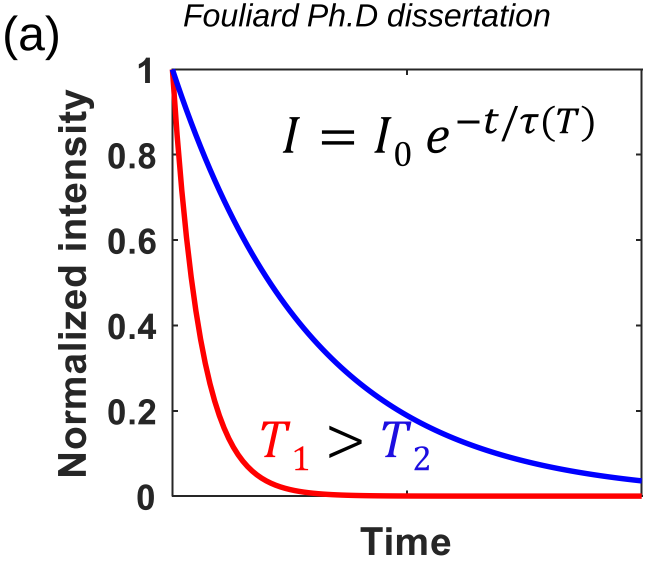

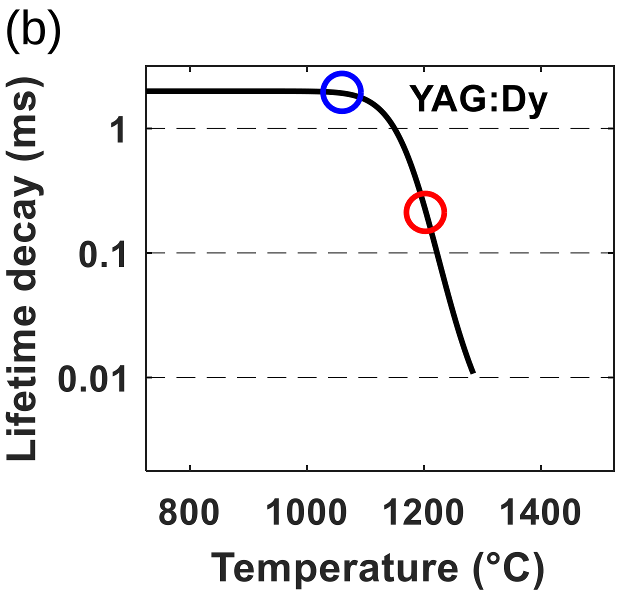

Schematic of (a) Normalized intensity vs. time for temperature T_1 and T_2, (b) correlating decay time with temperature

Luminescence lifetime decay:

$$\tau = \frac{1}{W_r + W_{nr}}$$

τ: lifetime decay,
$W_{r/nr}$: radiative and non-radiative deexcitation rates.

- Thermal quenching accelerates decay due to higher probability of vibrational deexcitation. Knappe, C. *PhD dissertation Lund University* (2013)

Absolute sensitivity:

$$S_a = \left| \frac{dQ}{dT} \right|$$

Q: sensor variable (τ or R),
T: temperature

- Higher sensitivity of the decay method in comparison with the intensity ratio method but often limited to a reduced temperature range. Heeg, et al. *AIP Conference Proceedings, Vol. 1552*, (2013)

Instrumentation developed for synchronized luminescence decay collection

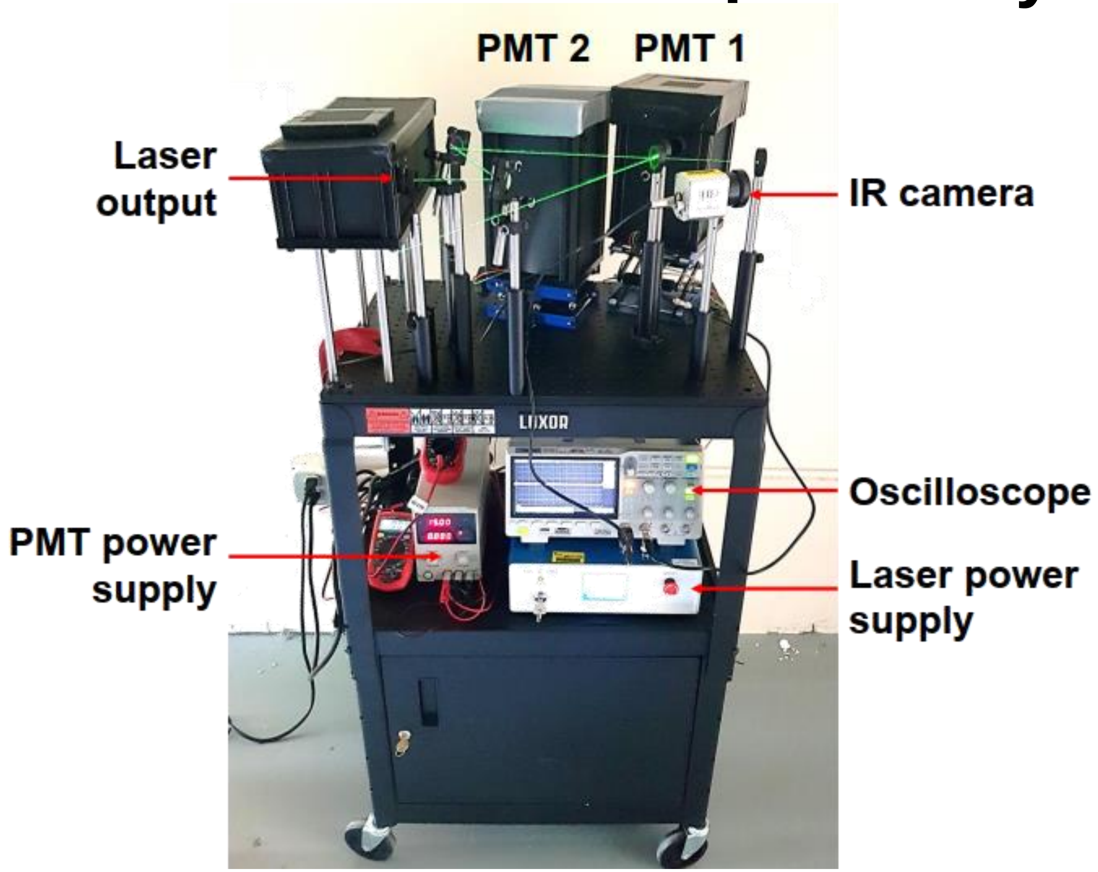

Fouliard et al., *Measurement Science & Technology*, 2020

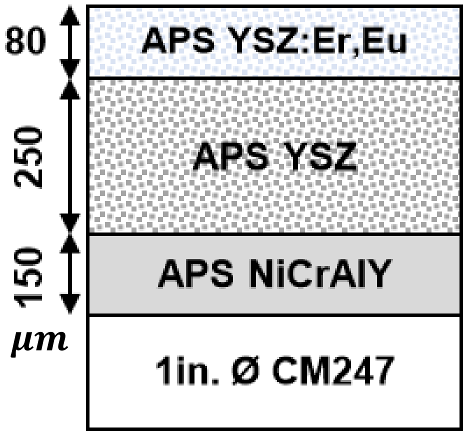

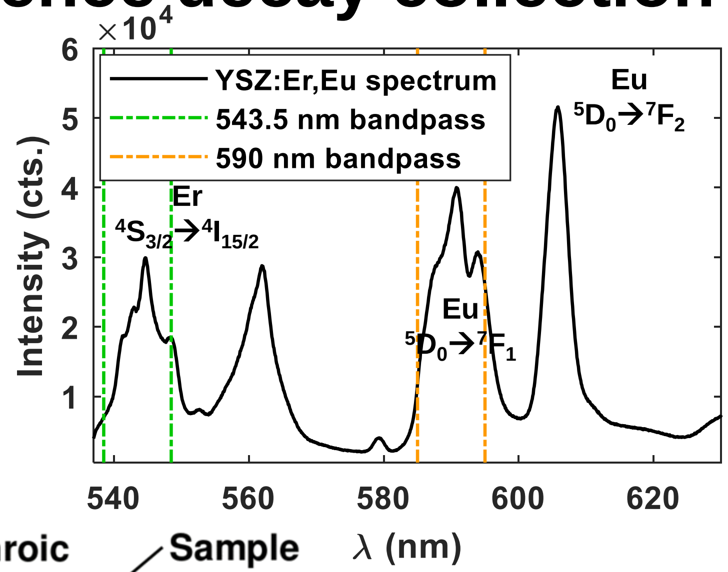

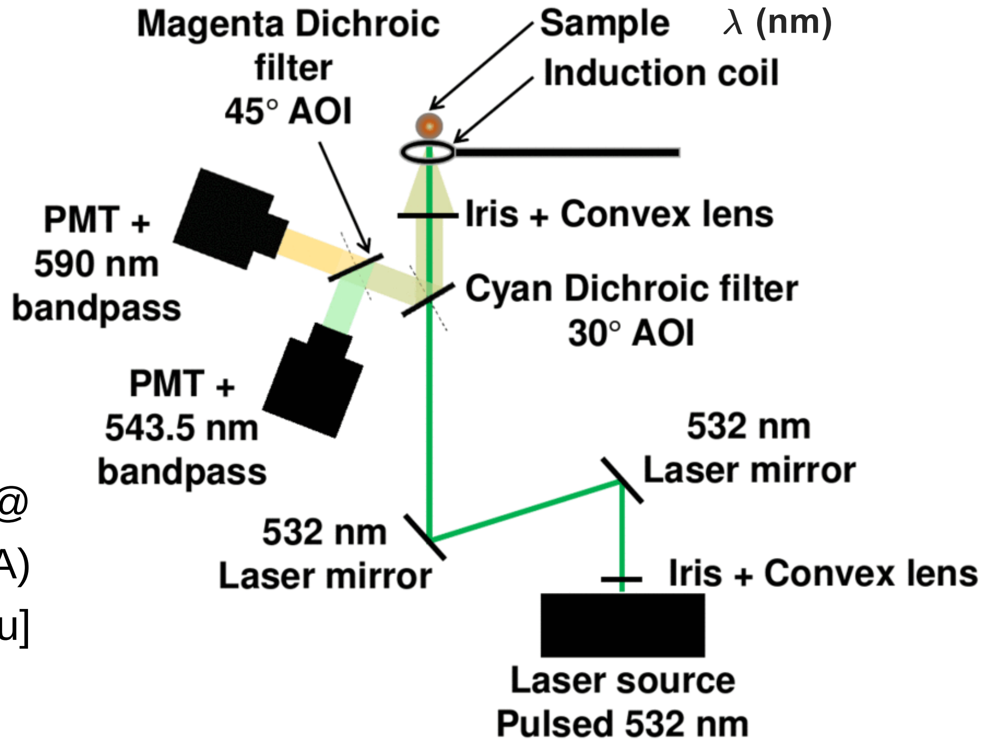

Parameters:

Nd:YAG 532 nm
0.5 mJ pulse
10 Hz
20 ns pulse duration

Sample:

Air Plasma Spray (UCF team @ FIT, Melbourne, FL, USA)
YSZ:Er,Eu [1.5% Er, 3% Eu] (Phosphor Technology, UK)
Annealed 2h @ 800˚C

Extension of temperature range vs. state-of-the-art

- Luminescence of Europium is quenched rapidly past 500°C, for high sensitivity measurements up to 850°C where reaching detector response limit.
- Temperature range extended by collecting the ratio of the normalized intensity variation Erbium/Europium.

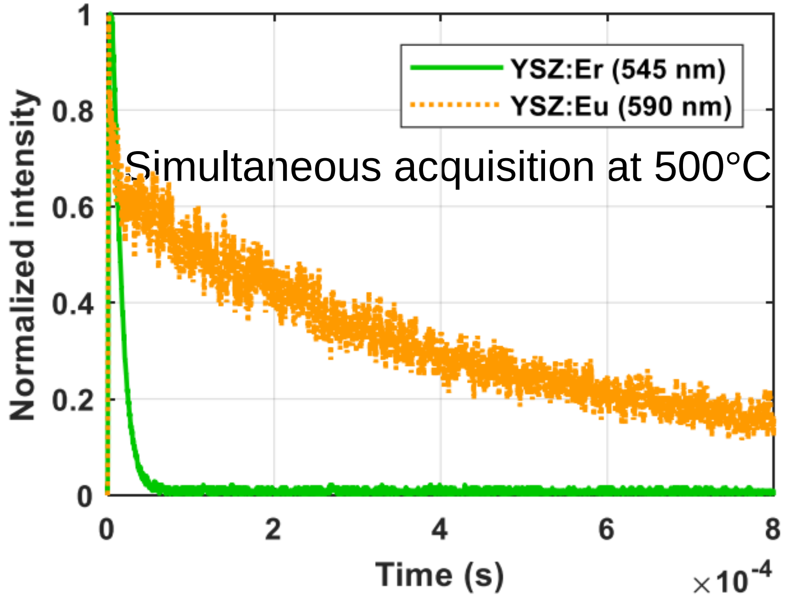

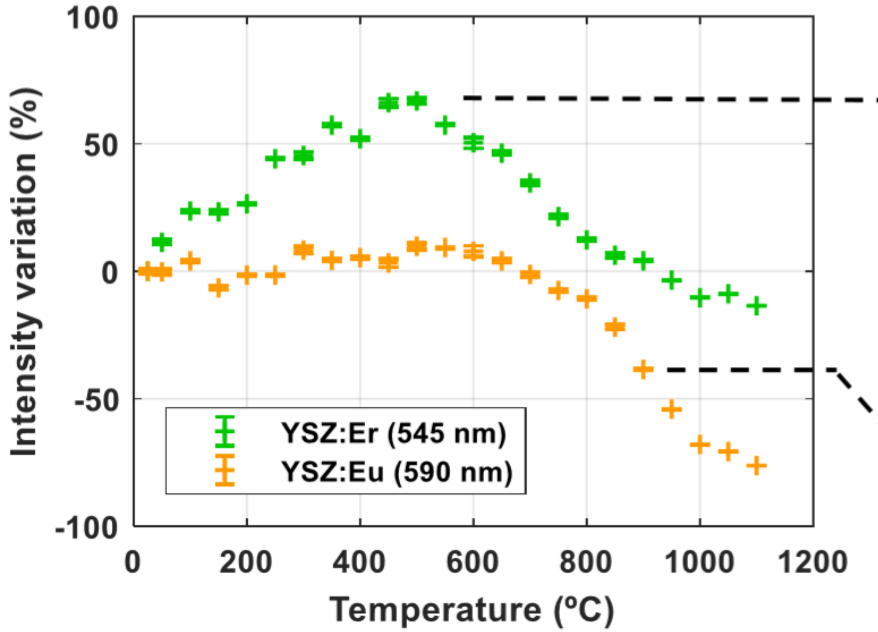

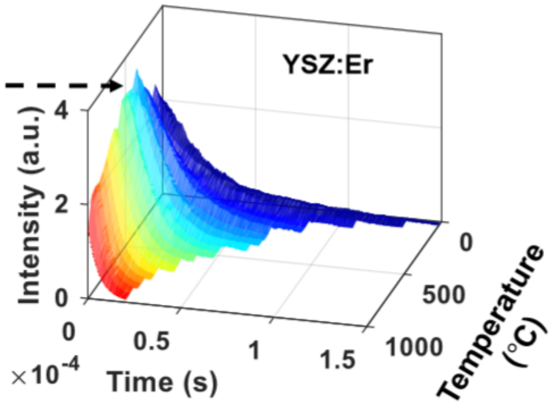

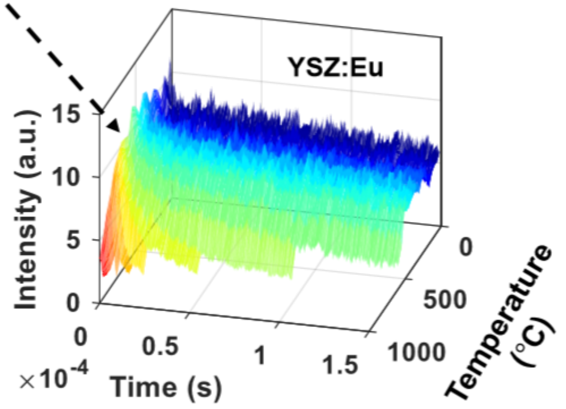

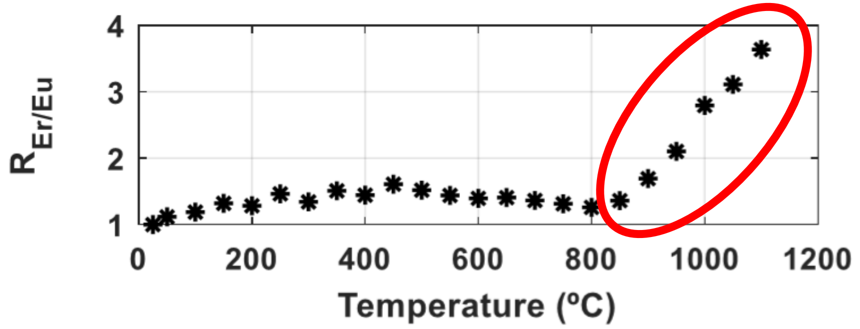

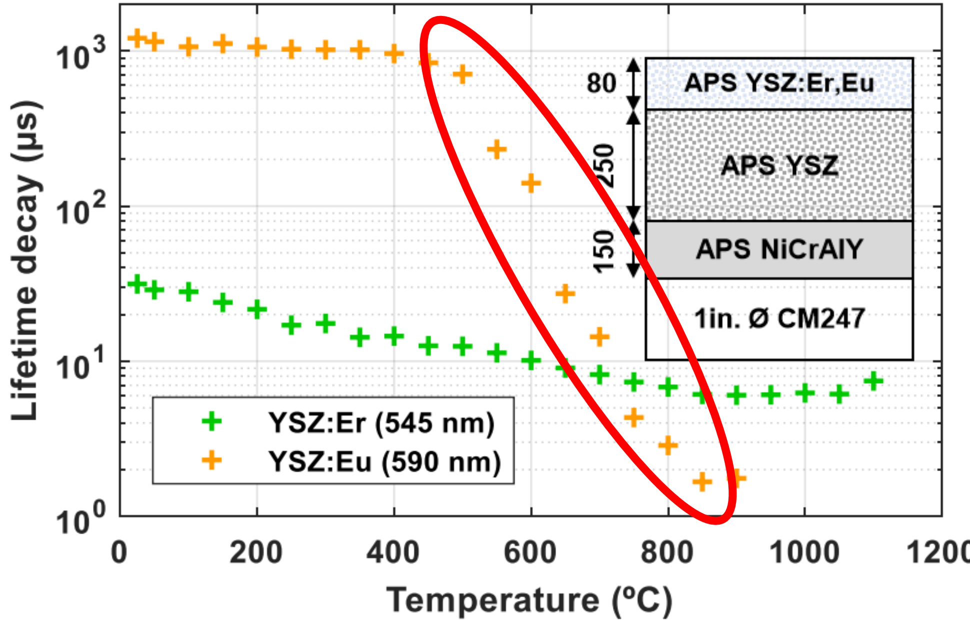

Fouliard et al., *Measurement Science & Technology*, 2020

Instrumentation developed for sub-surface temperature measurements

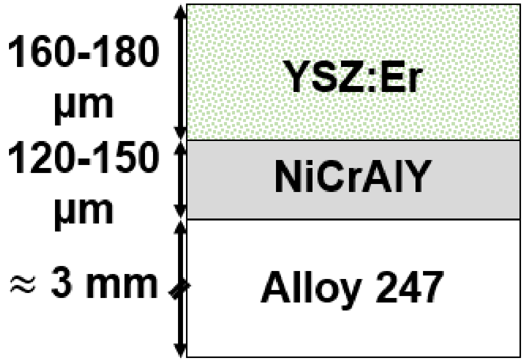

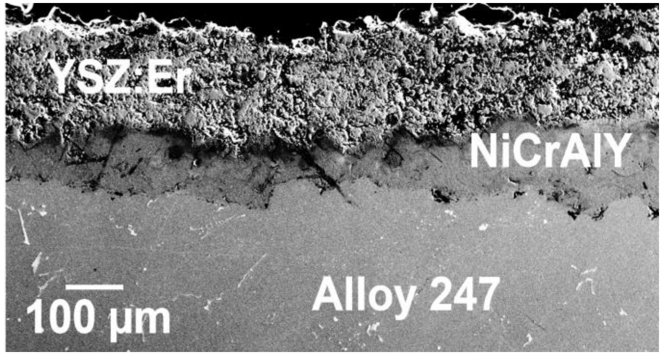

Parameters:

Nd:YAG 532 nm

0.5 mJ pulse

10 Hz

20 ns pulse duration

Sample:

Air Plasma Spray (UCF team @ FIT, Melbourne, FL, USA)

YSZ:Er [1.5% Er] (Phosphor Technology, UK)

Annealed 2h @ 800˚C

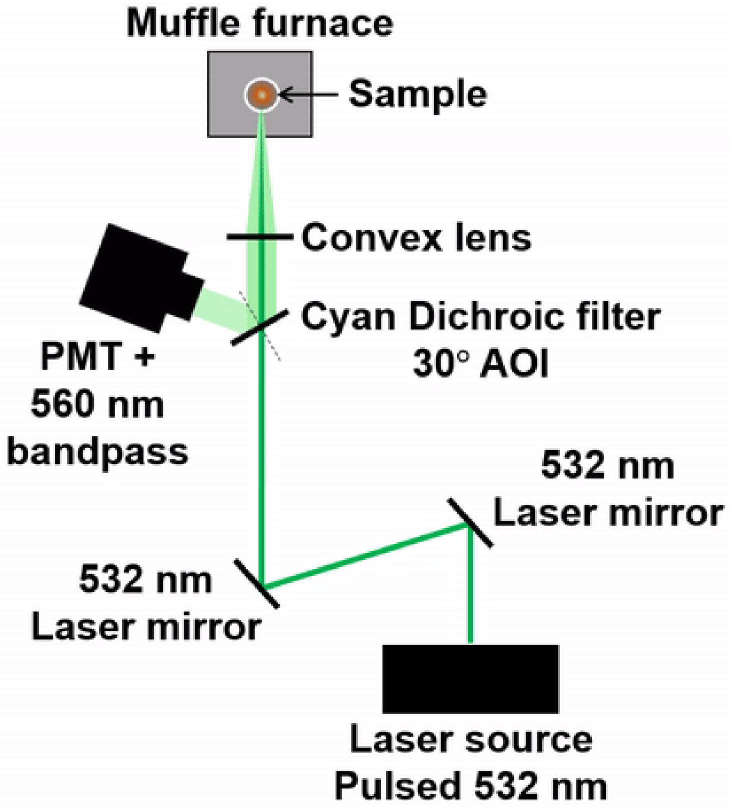

$$R^{thermal} = \sum R^{thermal}_{topcoat} + R^{thermal}_{bondcoat} + R^{thermal}_{substrate}$$

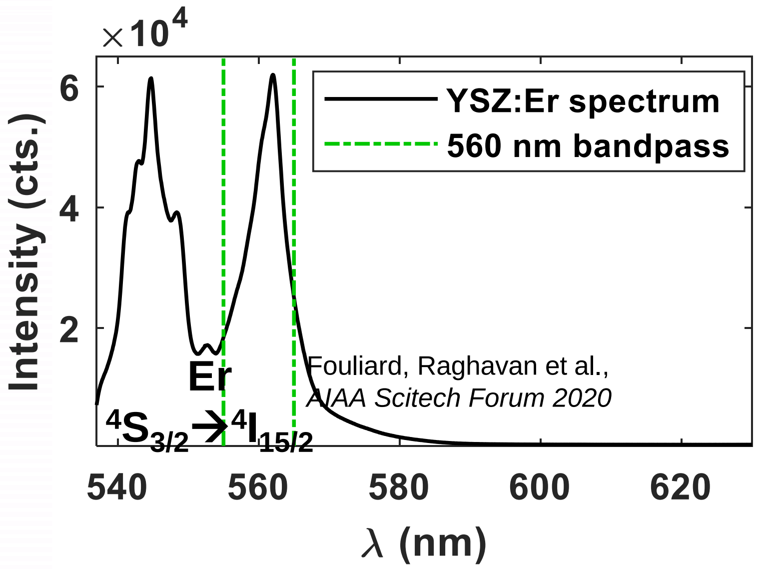

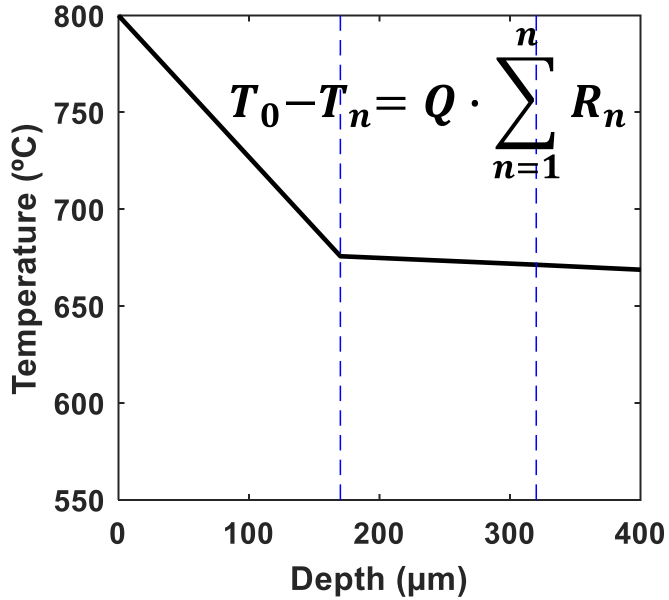

Determination of reference decays: isothermal case

- Calibration of the sensor response is achieved using a furnace that includes through holes for thermocouple and luminescence measurements
- Fit: Temperature-dependent multi-phonon relaxation model for the $^4S_{3/2} \rightarrow {}^4I_{15/2}$ transition combined with a model to account for the other thermally populated levels

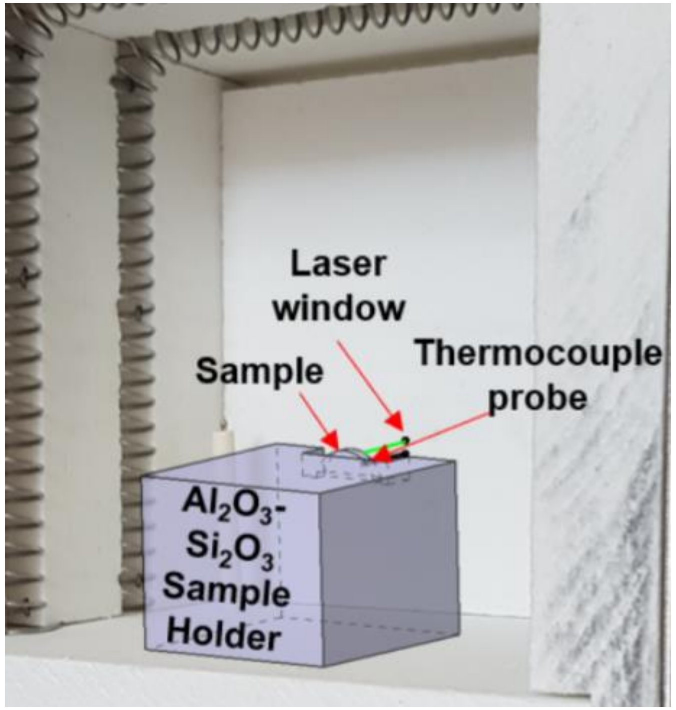

Inside view

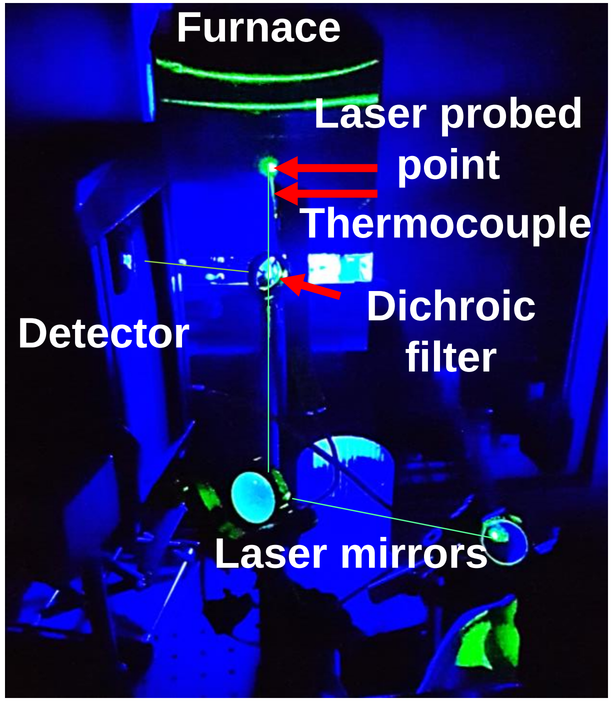

Outside view

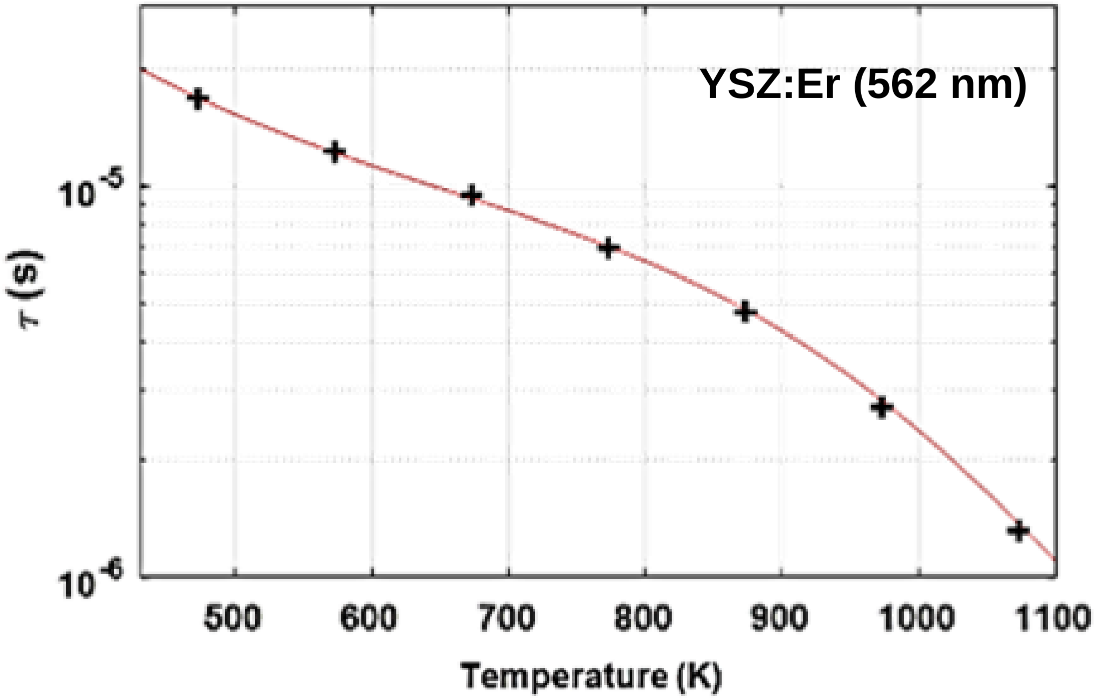

New method proposed for Phosphor Thermometry for sub-surface measurements
Sub-surface temperature point was successfully measured

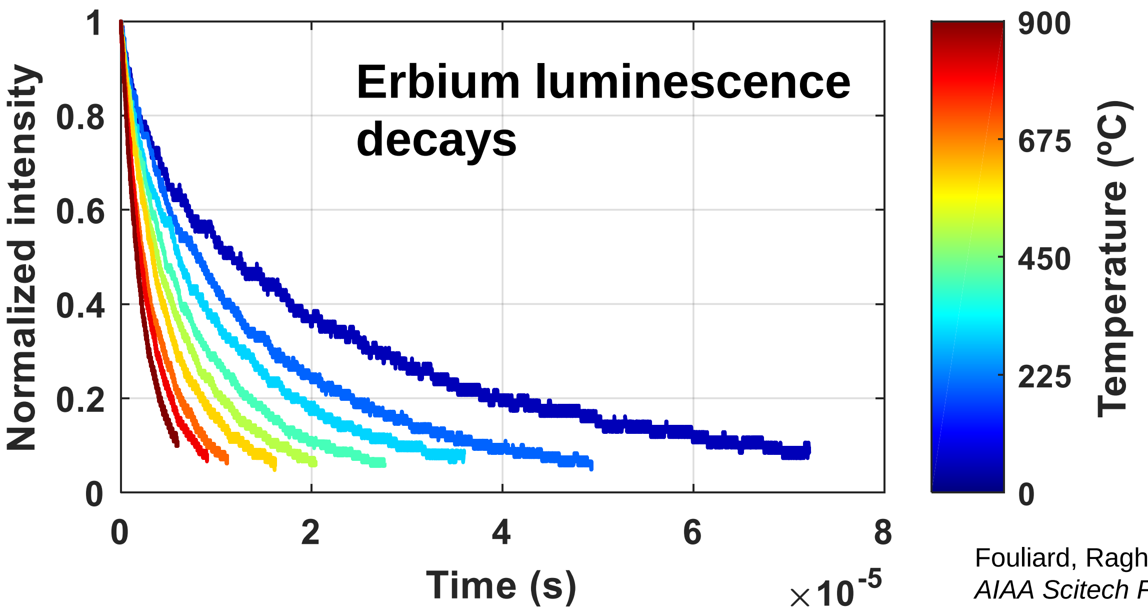

Fouliard, Raghavan et al., *AIAA Scitech Forum 2020*

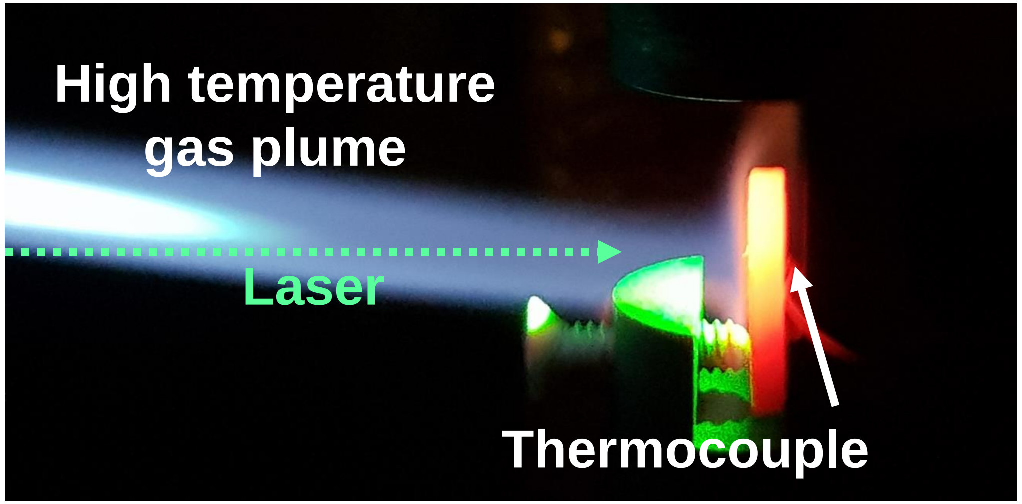

Model sub-surface location prediction for the temperature measurement:

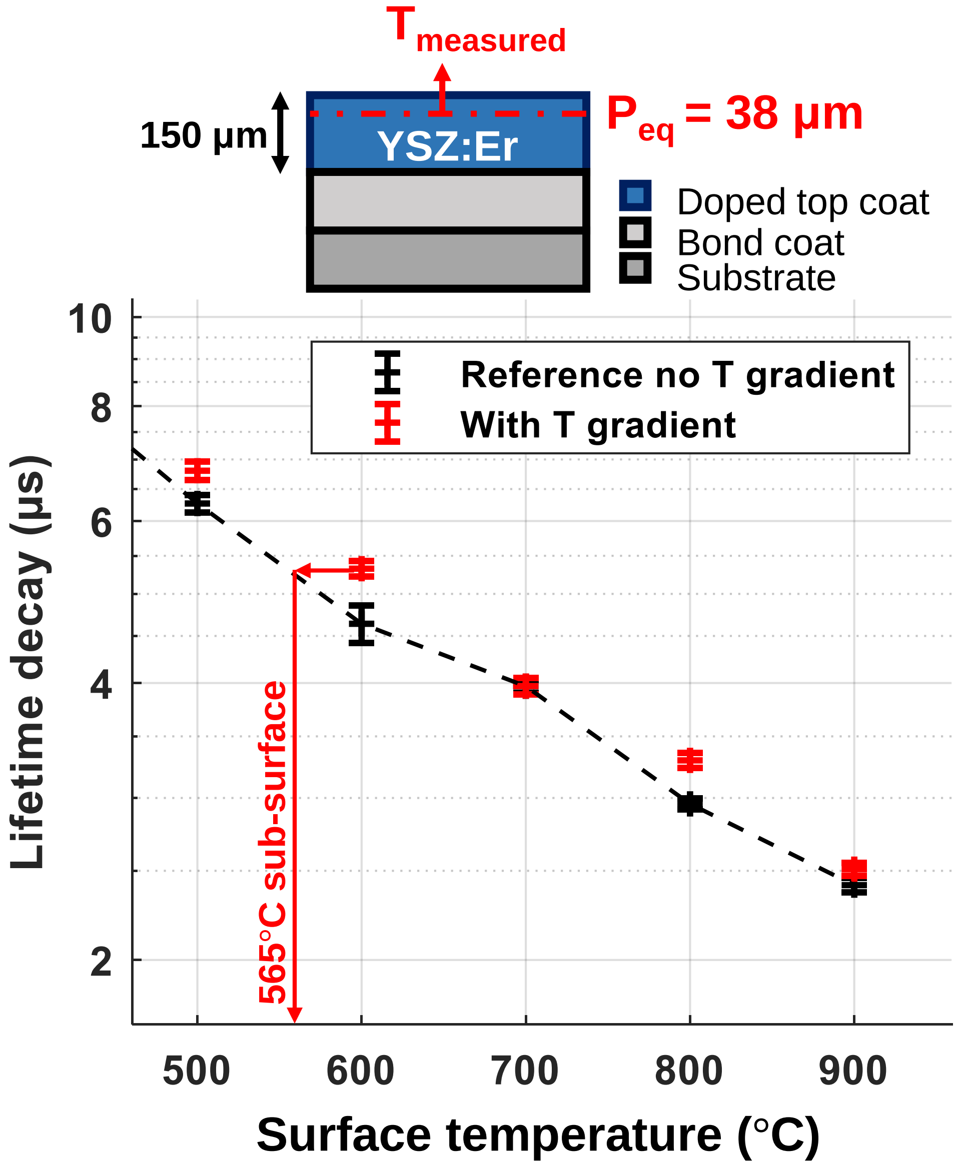

Coating damage monitoring

Part of tasks 3 & 4

Modeling delamination

Q. Fouliard, R. Ghosh, S. Raghavan *Surface and Coatings Technology* (2020): 126153.

Diffuse external reflectivity

$$\rho_0(n) = \frac{1}{2} + \frac{(3n+1)\cdot(n-1)}{6\cdot(n+1)^2} + \frac{n^2\cdot(n^2-1)^2}{(n^2+1)^3}\cdot \ln\left(\frac{n-1}{n+1}\right) - \frac{2n^3\cdot(n^2+2n-1)}{(n^2+1)\cdot(n^4-1)} + \frac{8n^4\cdot(n^4+1)}{(n^2+1)\cdot(n^4-1)^2}\cdot\ln(n)$$

Max diffuse internal reflectivity

$$\rho_{i,max}(n) = \left(1-\frac{1}{n^2}\right) + \frac{\rho_0(n)}{n^2}$$

Frustrated angle-averaged reflectivity

$$\overline{R}_f(d) = \frac{\int_0^{2\pi}\int_{\theta_c}^{\frac{\pi}{2}} \frac{\alpha\cdot\sinh^2(\beta\cdot d)}{1+\alpha\cdot\sinh^2(\beta\cdot d)}\cos\theta\cdot\sin\theta d\theta d\varphi}{\int_0^{2\pi}\int_{\theta_c}^{\frac{\pi}{2}}\cos\theta\cdot\sin\theta d\theta d\varphi}$$

$$\alpha_\perp = \frac{(n^2-1)^2}{4n^2\cdot\cos^2\theta\cdot(n^2\sin^2\theta-1)}$$

$$\alpha_\parallel = \alpha_\perp\cdot(\sin^2\theta\cdot(n^2+1)-1) \qquad \overline{R}_{f,unp} = \frac{\overline{R}_{f,\perp}+\overline{R}_{f,\parallel}}{2}$$

$$\beta = \frac{2\pi}{\lambda_0}\sqrt{n^2\cdot\sin^2\theta - 1}$$

$$\rho_i(d) = \overline{R}_{f,unp}(d)\cdot\left(1-\frac{1}{n^2}\right) + \frac{\rho_0(n)}{n^2}$$

Layer	**n**	$\rho_{i,max}$
Air	**1**	84%
Top coat	2.17	39%
TGO	1.76	
Top coat - Bond coat		4%

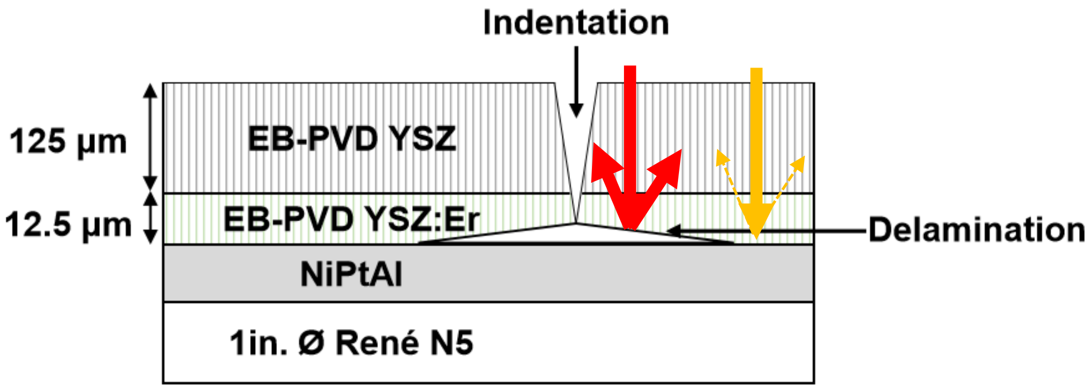

Model prediction of delamination-induced luminescence contrast

$$Y_\lambda(x) = [I_{t,\lambda}(x)\ J_{t,\lambda}(x)\ I_{m,\lambda}(x)\ J_{m,\lambda}(x)\ I_{b,\lambda}(x)\ J_{b,\lambda}(x)]^T$$

$$A_{z,\lambda} = \begin{pmatrix} -(K_{z,\lambda}+S_{z,\lambda}) & S_{z,\lambda} \\ -S_{z,\lambda} & K_{z,\lambda}+S_{z,\lambda} \end{pmatrix} \quad Q_z = \frac{1}{2}\begin{pmatrix} q_z K_{z,\ell} & q_z K_{z,\ell} \\ -q_z K_{z,\ell} & -q_z K_{z,\ell} \end{pmatrix}$$

$$\frac{dY_\ell(x)}{dx} = \begin{pmatrix} A_{t,\ell} & 0 & 0 \\ 0 & A_{m,\ell} & 0 \\ 0 & 0 & A_{b,\ell} \end{pmatrix} \cdot Y_\ell(x)$$

$$\frac{dY_\mathcal{L}(x)}{dx} = \begin{pmatrix} A_{t,\mathcal{L}} & 0 & 0 \\ 0 & A_{m,\mathcal{L}} & 0 \\ 0 & 0 & A_{b,\mathcal{L}} \end{pmatrix} \cdot Y_\mathcal{L}(x) + \begin{pmatrix} Q_t & 0 & 0 \\ 0 & Q_m & 0 \\ 0 & 0 & Q_b \end{pmatrix} \cdot Y_\ell(x)$$

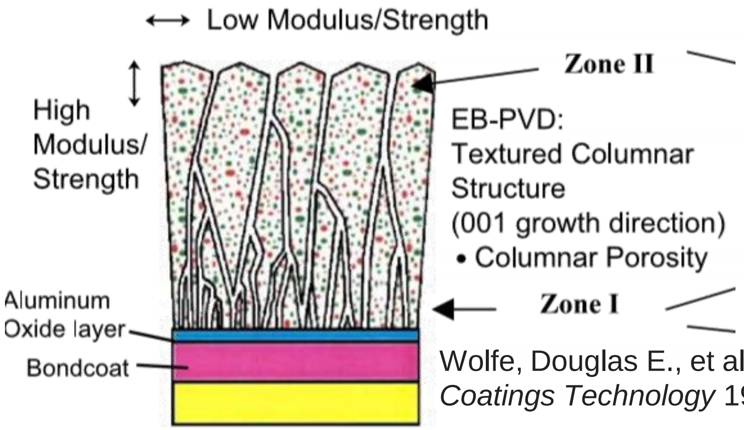

Wolfe, Douglas E., et al *Surface and Coatings Technology* 190.1 (2005): 132-149.

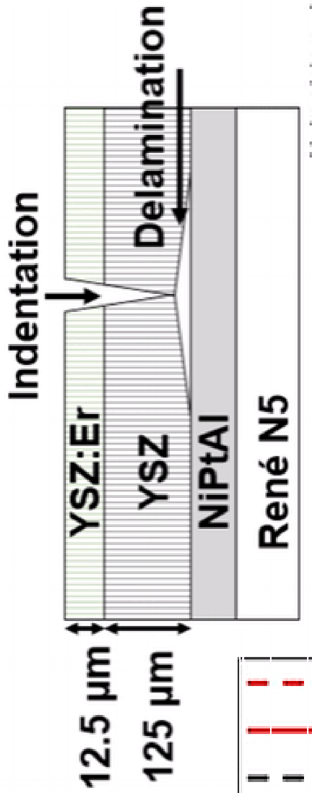

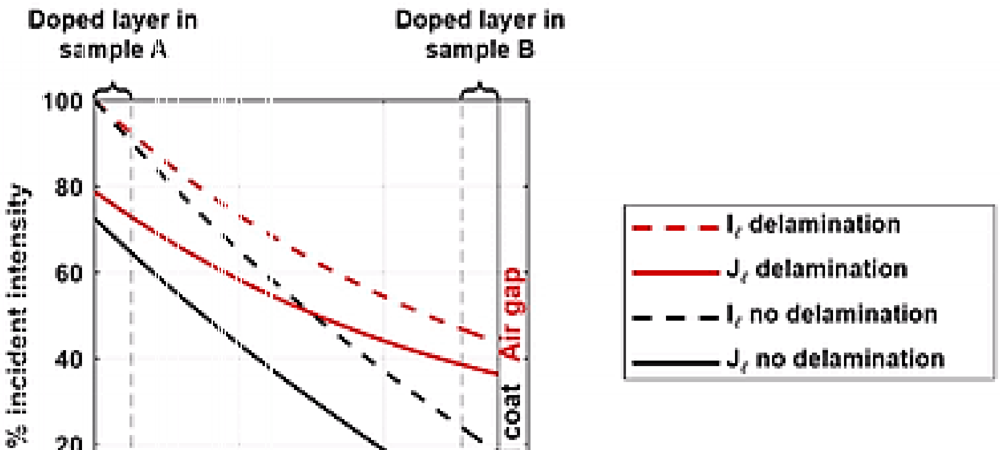

Q. Fouliard, R. Ghosh, S. Raghavan *Surface and Coatings Technology* (2020): 126153.

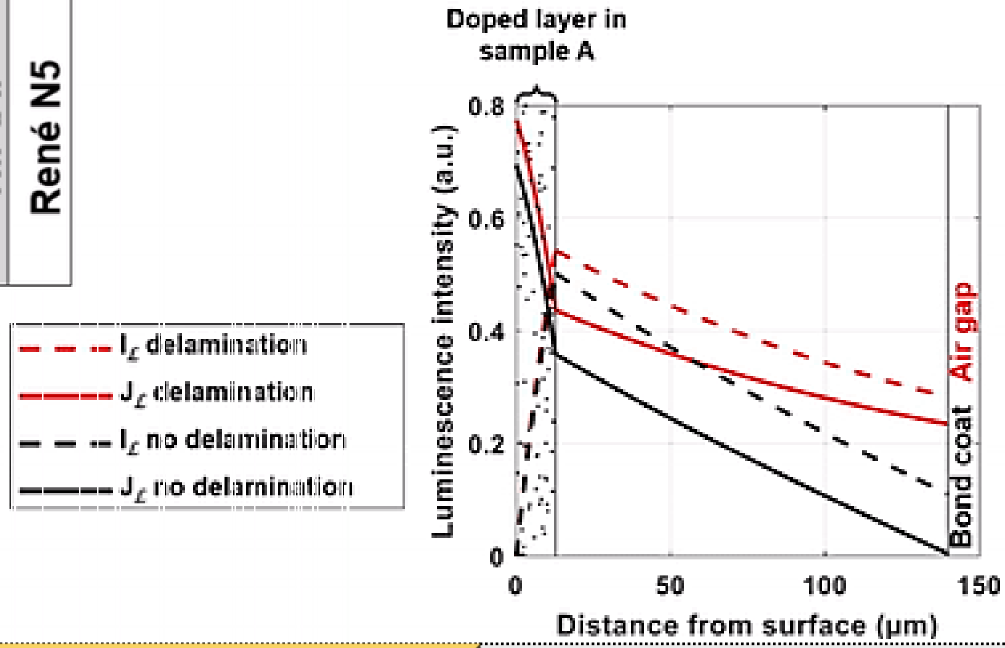

Delamination monitoring: Comparison experiment vs. model

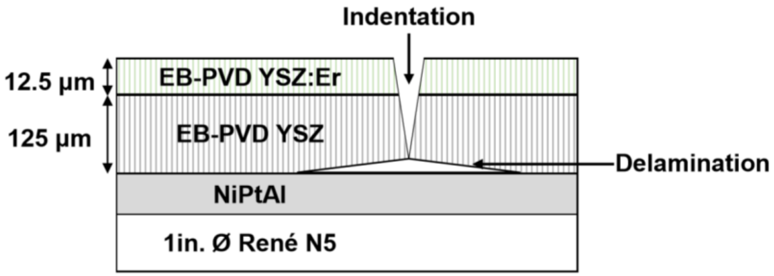

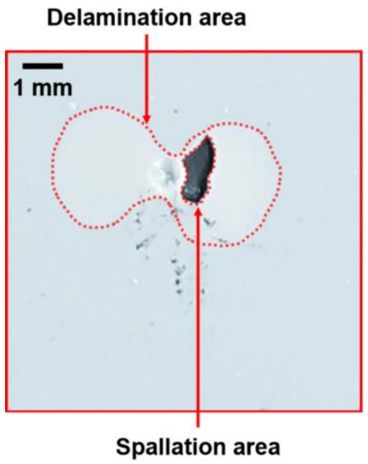

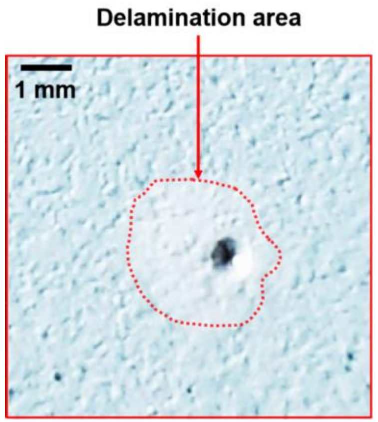

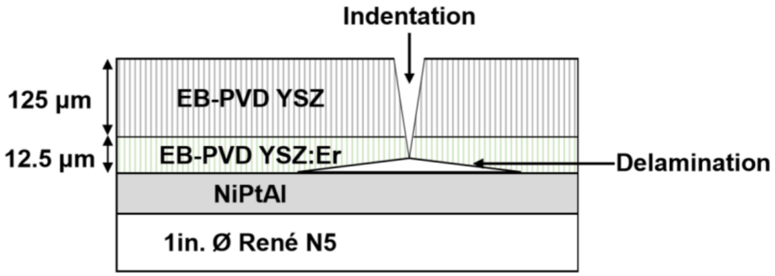

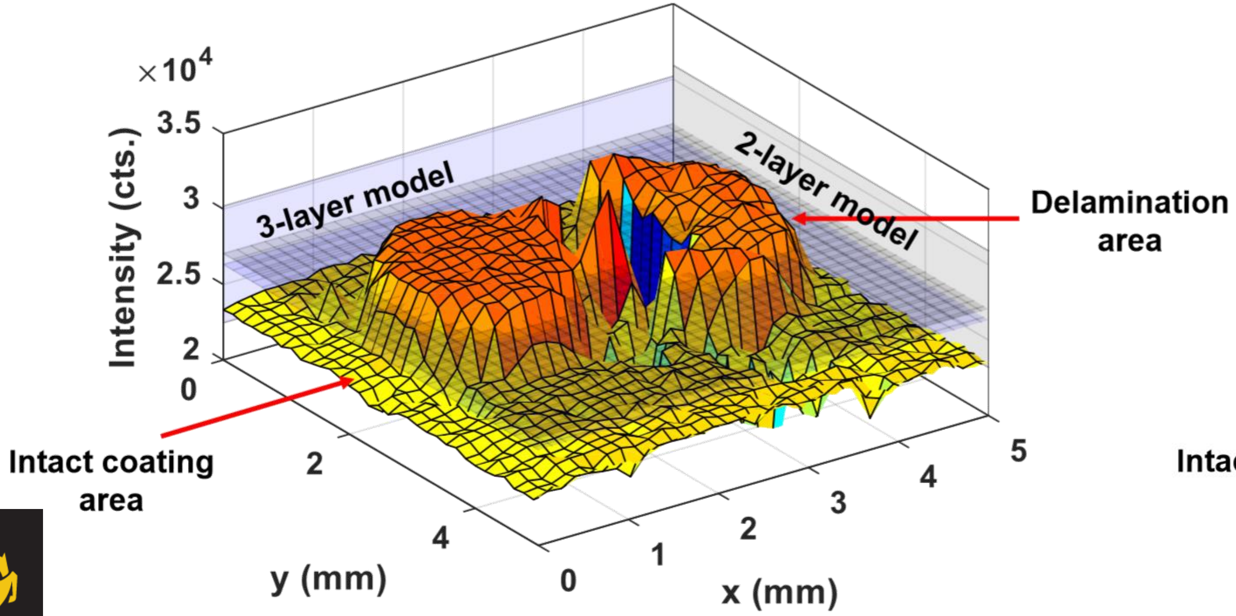

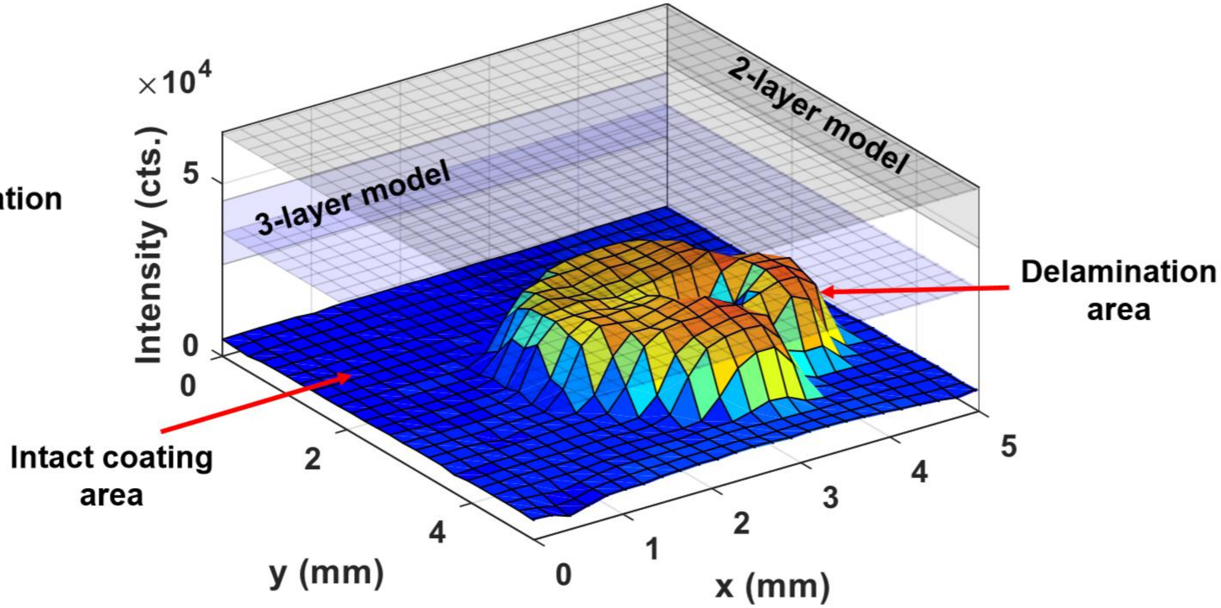

Q. Fouliard, R. Ghosh, S. Raghavan *Surface and Coatings Technology* (2020): 126153.

Delamination monitoring: Luminescence trade-off for delamination detection

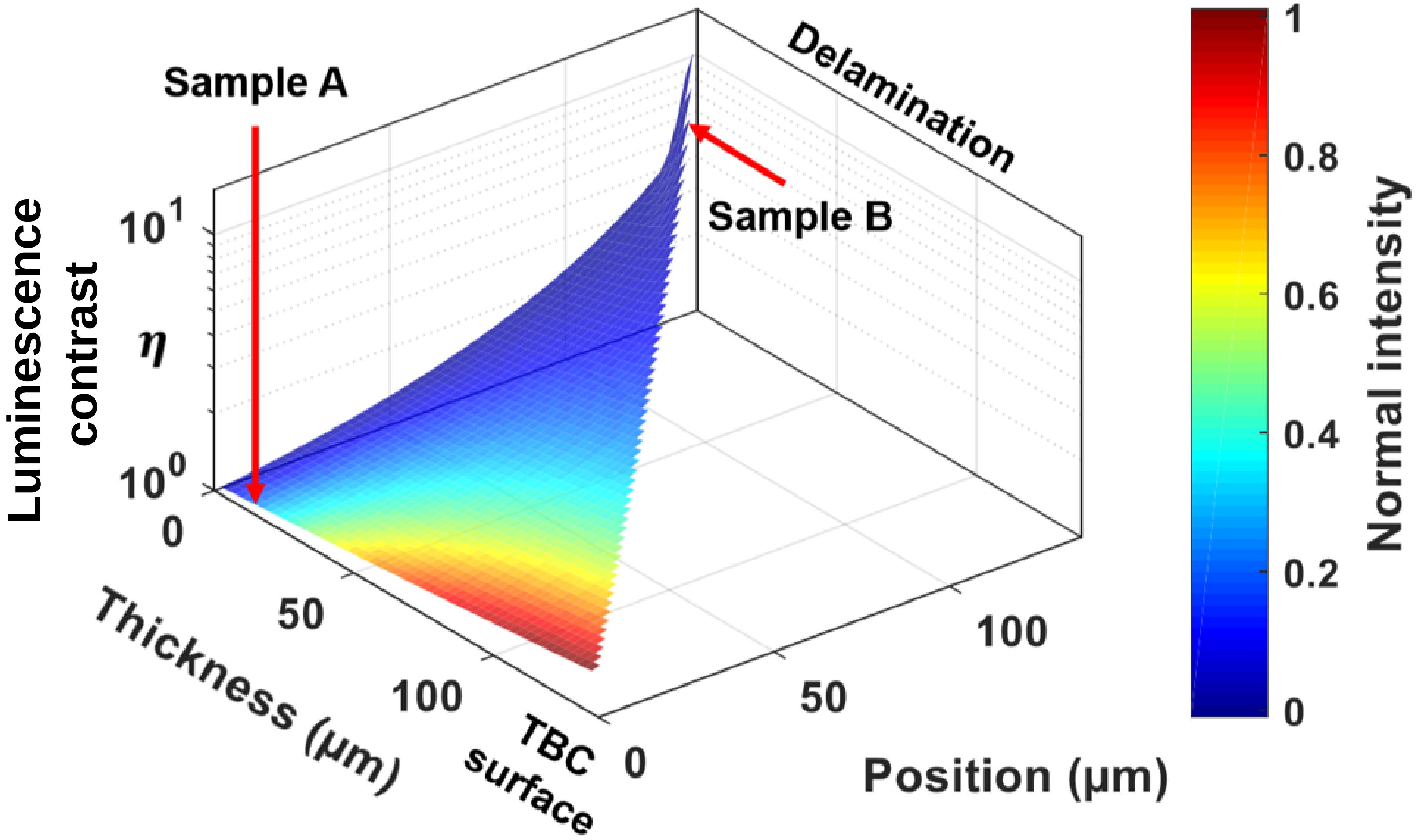

Q. Fouliard, R. Ghosh, S. Raghavan *Surface and Coatings Technology* (2020): 126153.

Conclusions & Perspectives

Conclusions

- Precise determination of temperatures in TBCs can result in large benefits in terms of fuel savings, reduction of emission, as well as better monitoring of TBC lifetime

- Enabled the extension of the range of measurable temperatures using Phosphor Thermometry with higher sensitivity by capturing simultaneously luminescence decays and intensities out of a co-doped YSZ:Er,Eu top layer.

- Improved sub-surface temperature measurements using TBC in the presence of a thermal gradient.

- Enabled accurate determination of delamination in coatings through a novel modeling approach, validated with experiments.
  - For the first time, a configuration with a thin sensing layer placed at the top surface was able to track an underlying delamination area (located below a thick YSZ intermediate layer) with high luminescence intensity for fast acquisition.
  - Sensor TBC configuration can be optimized for erosion and delamination tracking using the results of the model.

Future work

- Additional synchrotron experiments for rare-earth doped EB-PVD TBC strain measurements to further establish the effects of rare-earth dopant addition to coating strains (collaboration: GE Research, Argonne National Lab).

- Model adaptation and experimentation using high-emissivity paints for improved temperature measurements on painted TBCs (collaborator: GE Aviation).

Provided acceptance of extension proposal

- Adaptation of the instrumentation to operate on a combustor / turbine section (the current project successfully demonstrated lab-scale functionality as planned – the existing built-up could now be adapted to rapidly increase its technology readiness level).

Publications

- Quentin Fouliard, Ranajay Ghosh, Seetha Raghavan, "Quantifying thermal barrier coating delamination through luminescence modeling", Surface and Coatings Technology, 126153, 2020
- Quentin Fouliard, Johnathan Hernandez, Bauke Heeg, Ranajay Ghosh, Seetha Raghavan, "Phosphor Thermometry Instrumentation for Synchronized Acquisition of Luminescence Lifetime Decay on Thermal Barrier Coatings", Measurement Science and Technology 31(5), 054007, 2020
- Quentin Fouliard, Sandip Haldar, Ranajay Ghosh, and Seetha Raghavan. "Modeling luminescence behavior for phosphor thermometry applied to doped thermal barrier coating configurations." Applied Optics 58(13), D68-D75, 2019
- Quentin Fouliard, Ranajay Ghosh, Seetha Raghavan, "Doped 8% Yttria-Stabilized Zirconia for Temperature Measurements on Thermal Barrier Coatings using Phosphor Thermometry", 2020 AIAA SciTech Forum, Orlando, FL, January 6-10, 2020
- Sandip Haldar, Peter Warren, Quentin Fouliard, David Moreno, Mary McCay, Jun Sang Park, Peter Kenesei, Jonathan Almer, Ranajay Ghosh, Seetha Raghavan, "Synchrotron XRD measurements of Thermal Barrier Coating Configurations With Rare Earth Elements For Phosphor Thermometry", Proceedings of ASME Turbo Expo 2019: Turbine Technical Conference and Exposition GT2019, Phoenix, AZ, June 17-21, 2019
- Quentin Fouliard, Sanjida A. Jahan, Lin Rossmann, Peter Warren, Ranajay Ghosh, Seetha Raghavan, "Configurations for Temperature Sensing of Thermal Barrier Coatings," 1st International Conference on Phosphor Thermometry (ICPT 2018), Glasgow, UK, July 25-27, 2018

Patents

- Quentin Fouliard, Ranajay Ghosh, Seetha Raghavan, "Phosphor Thermometry System for Synchronized Luminescence Lifetime Decay Measurements", U.S.Patent Serial No. 62/944,390,12/2019
- Quentin Fouliard, Ranajay Ghosh, Seetha Raghavan, "Rare-Earth Doped Thermal Barrier Coating Bond Coat for Thermally Grown Oxide Luminescence Sensing", U.S.Patent Serial No. 62/940,963,11/2019

Acknowledgments

Collaborators

Lumium — Bauke Heeg

Florida Institute of Technology — Mary McCay, Frank Accornero, David Moreno

Argonne National Laboratory — Jonathan Almer, Jun Sang-Park

GE — Ed Hoffmann, Joshua Salisbury

NASA — Jeffrey Eldridge

SIEMENS — Dr. Ramesh Subramanian

This material is based upon work supported by the U.S. Department of Energy, National Energy Technology Laboratory, University Turbine Systems Research (UTSR) under Award Number: DE-FE0031282.

THANK YOU FOR YOUR ATTENTION

CONTACT EMAILS AND WEBSITE

seetha.raghavan@ucf.edu
quentin@knights.ucf.edu

https://aerostructures.cecs.ucf.edu/

ANNEX

Modeling Luminescence Intensity

Four-flux Kubelka-Munk model to account for scattering and absorption of light

$$Y_{laser}(x) = \begin{pmatrix} I_{laser}(x) \\ J_{laser}(x) \end{pmatrix} \qquad Y_{lum}(x) = \begin{pmatrix} I_{lum}(x) \\ J_{lum}(x) \end{pmatrix}$$

I_{laser} : intensity of incident laser traveling towards bond coat
J_{laser} : intensity of scattered laser traveling towards top surface
I_{lum} : intensity of the luminescence traveling towards bond coat
J_{lum} : intensity of the luminescence traveling towards top surface

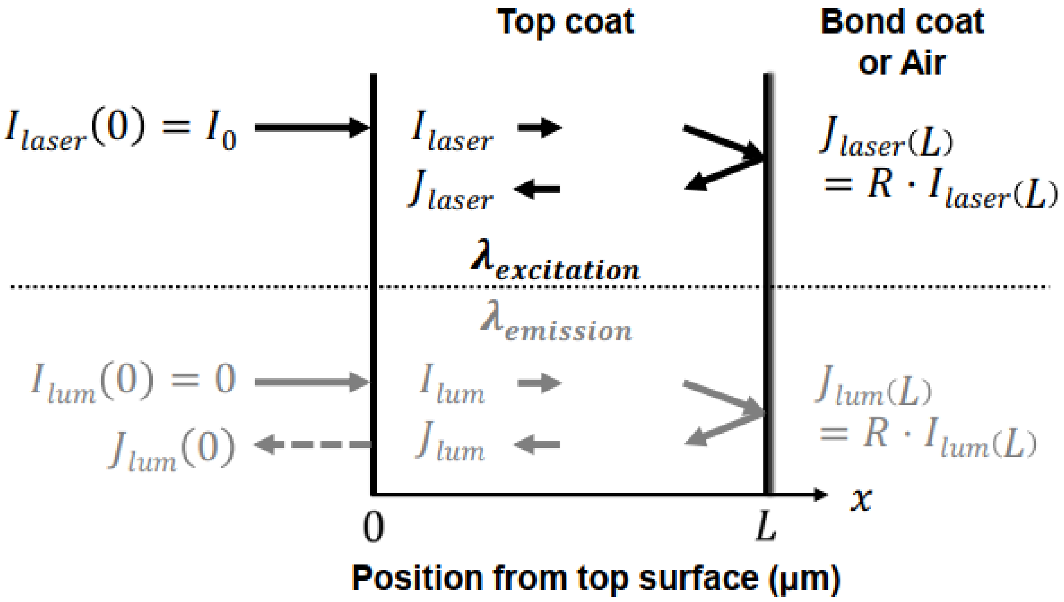

$$\frac{dY_{laser}(x)}{dx} = AY_{laser}(x)$$

$$\frac{dY_{lum}(x)}{dx} = AY_{lum}(x) + QY_{laser}(x)$$

$$S \equiv 2s$$

$$K \equiv 2k.$$

s: scattering coefficient
k: absorption coefficient
q: quantum efficiency

$$A_{laser} = \begin{pmatrix} -(K_{laser} + S_{laser}) & S_{laser} \\ -S_{laser} & K_{laser} + S_{laser} \end{pmatrix}$$

$$A_{lum} = \begin{pmatrix} -(K_{lum} + S_{lum}) & S_{lum} \\ -S_{lum} & K_{lum} + S_{lum} \end{pmatrix} \qquad Q = \begin{pmatrix} \frac{qK_{laser}}{2} & \frac{qK_{laser}}{2} \\ -\frac{qK_{laser}}{2} & -\frac{qK_{laser}}{2} \end{pmatrix}$$

λ (nm)	s (m^{-1})	k (m^{-1})
355 (exc. Dy)	50866	511
532 (exc. Er, Sm)	33026	111
545 (em. Er)	32113	107
590 (em. Dy)	29585	95
619 (em. Sm)	28685	90

Scattering and absorption coefficients / Excitation and emissions wavelengths used for the modeling study

Modeling Luminescence Intensities – Results of Kubelka-Munk model

Fouliard, Quentin, et al. "Modeling luminescence behavior for phosphor thermometry applied to doped thermal barrier coating configurations." Applied optics 58.13 (2019): D68-D75.

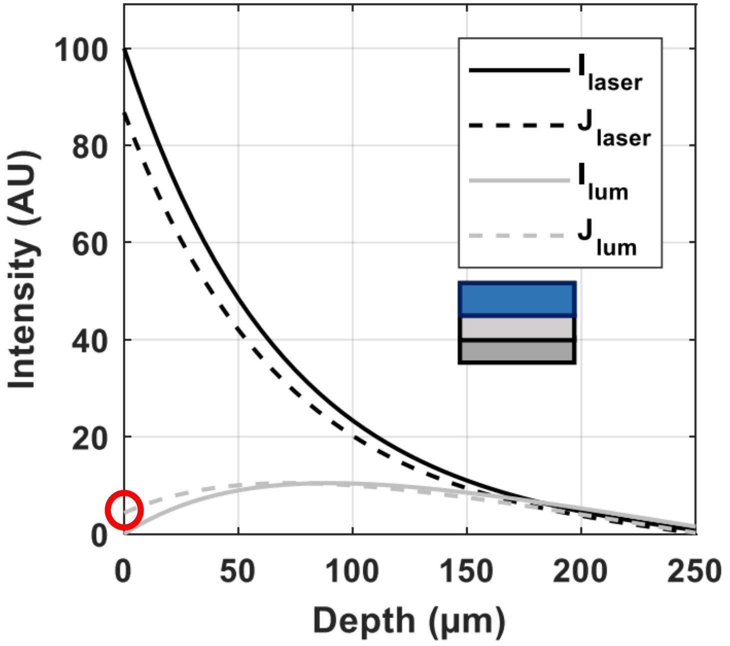

(C1) Fully doped coating

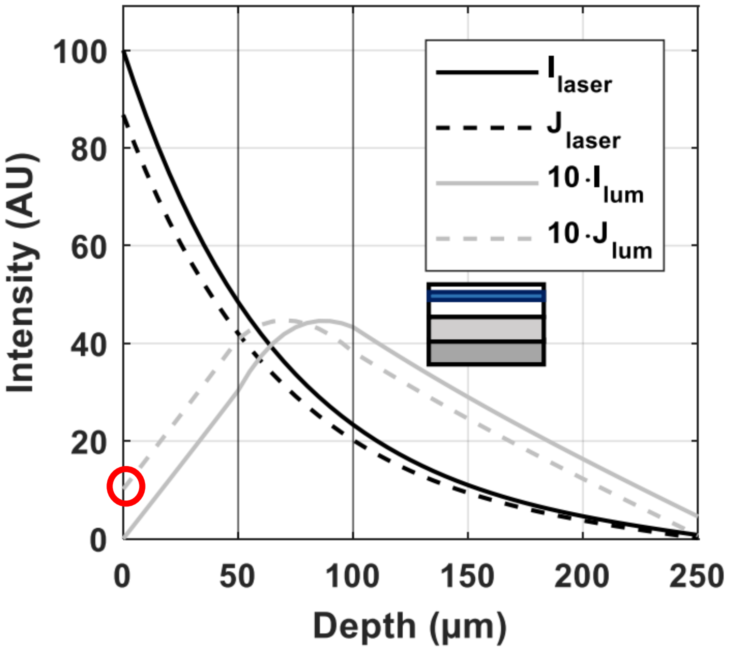

(C2) Embedded layer of doped YSZ

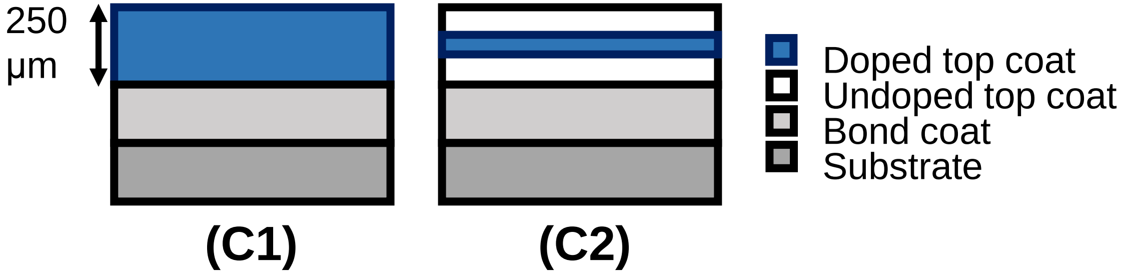

(C1): 250μm thick doped layer

(C2): 50μm thick doped layer buried at 50 μm

Collectable luminescence intensity	$J_{lum}(0)$
(C1)	4.3
(C2)	1.0

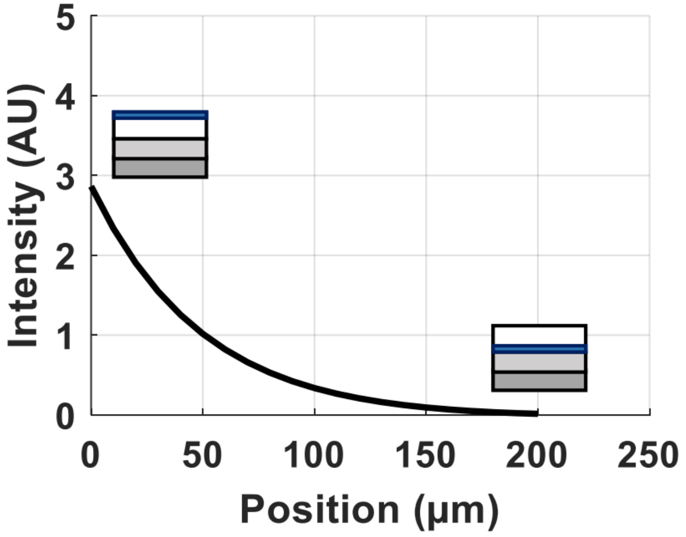

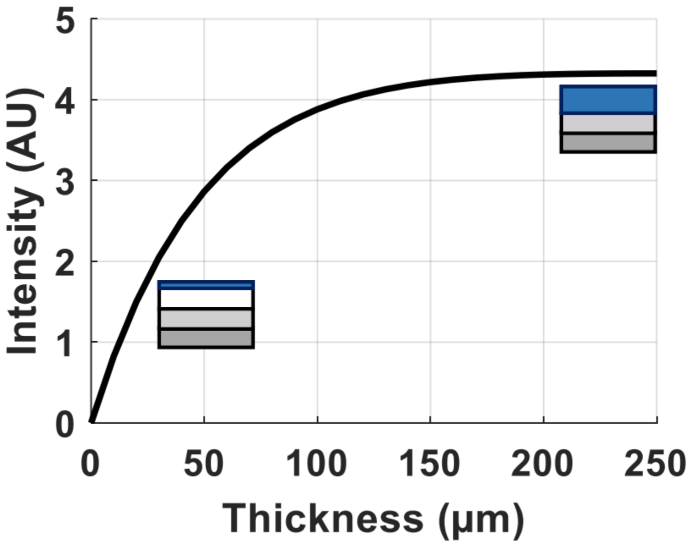

Luminescence decay behavior in doped TBC configurations

Modified Kubelka-Munk model

- Phosphor Thermometry based on the decay method is more sensitive to temperature variation than intensity-based methods.
- Classical Kubelka-Munk model provides only luminescence intensity distributions.
- Modeling decay is therefore important to understand the effect of TBC configurations.
- I developed a modified Kubelka-Munk model to predict decay behavior of the luminescence:

$$\phi = e^{-t/\tau(x)}$$

$$\frac{dY_{lum}(x,t)}{dx} = A_{lum} Y_{lum}(x,t) + \phi Q Y_{laser}(x)$$

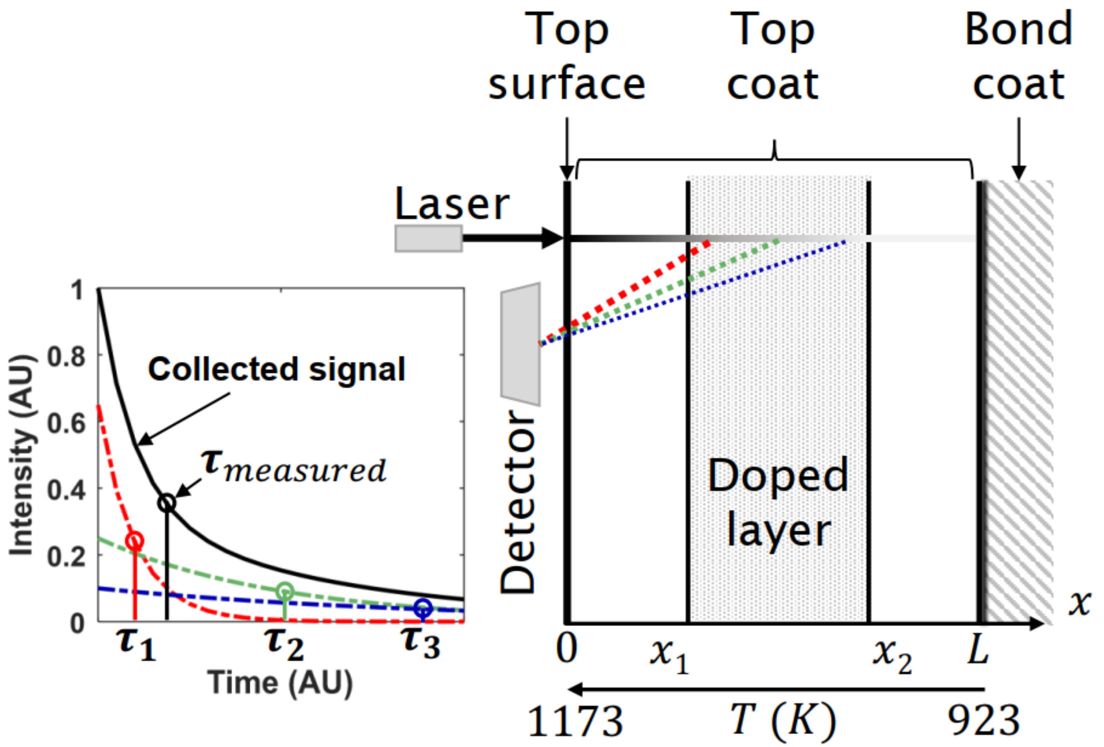

- A gradient of temperature exists in real operating conditions.
- The emerging luminescence is a convoluted signal coming from all the locations in the doped layer.

Fouliard, Q., et al. *Applied optics* 58.13 (2019): D68-D75.

Luminescence decay behavior in doped TBC configurations

Modified Kubelka-Munk model

$$\phi = e^{-t/\tau(x)}$$

$$\frac{dY_{lum}(x,t)}{dx} = A_{lum}Y_{lum}(x,t) + \phi Q Y_{laser}(x)$$

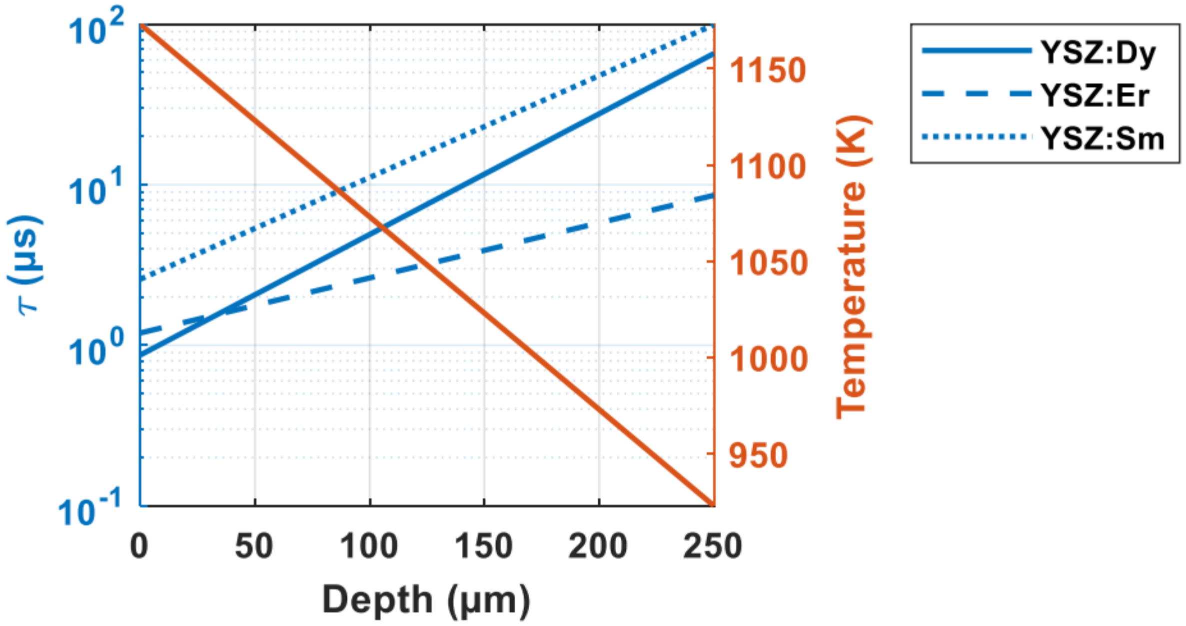

- The gradient of temperature can be calculated using thermal conductivities of the materials.
- The function $\tau(x)$ is determined from the temperature distribution across the coating, $\mathrm{T}(x)$
- The objective of the modified model is to predict the equivalent position – indicating at which depth the Phosphor Thermometry system is making its measurement.

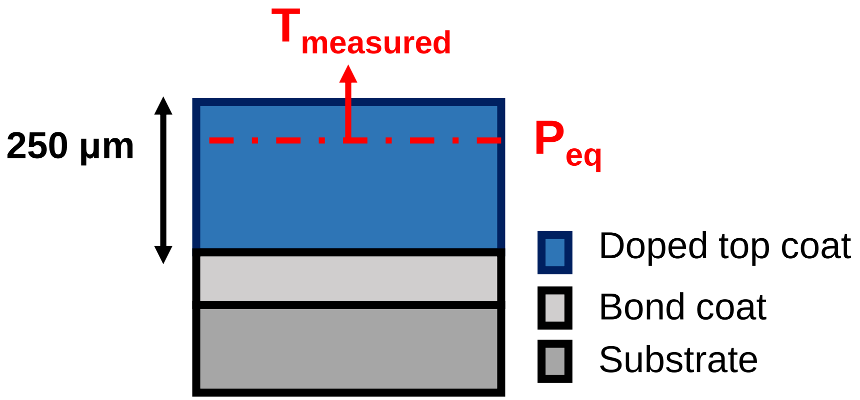

Fouliard, Q., et al. *Applied optics* 58.13 (2019): D68-D75.

Luminescence decay behavior in doped TBC configurations

Extension of Kubelka-Munk model - Results

- The decay constant fitted for any configuration can be associated with a particular position of the top coating.
- The decay constant is found to match with that of the luminescence generated at 37 μm in-depth for (C1).
- In case of TBC with a doped layer (C2) of thickness 50 μm and positioned at 50 μm, the decay constant is the same as the luminescence from a position of depth 69 μm.

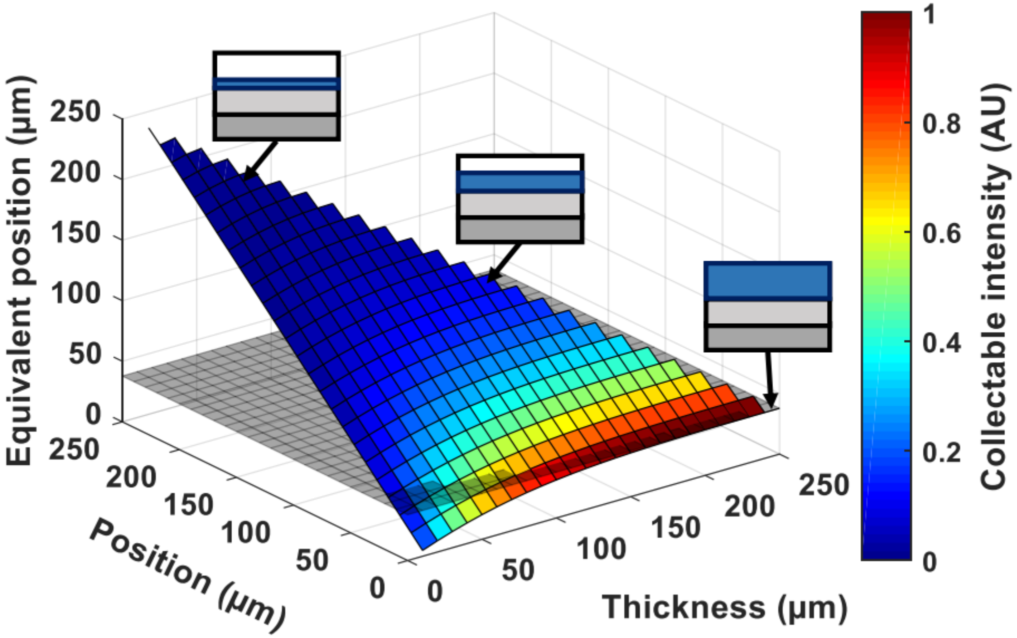

Results for YSZ:Dy for 325 doped TBC configurations (resolution 10 μm)

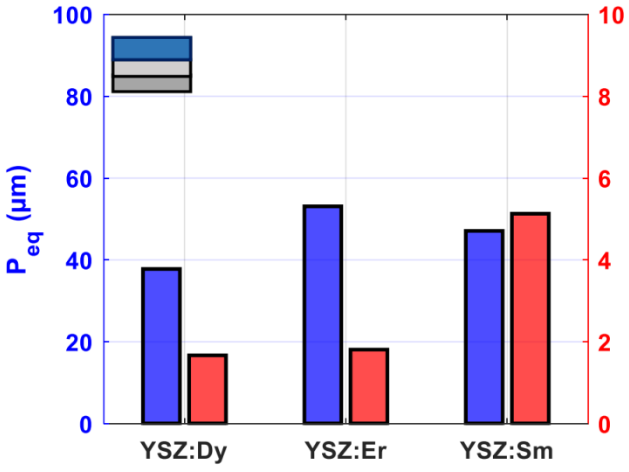

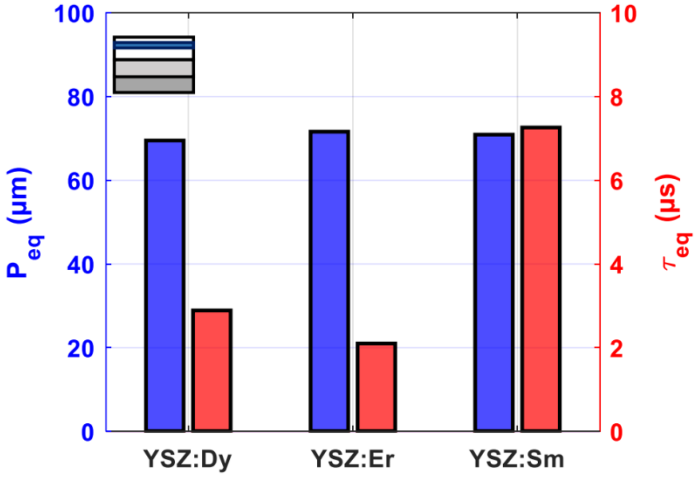

Fouliard, Q., et al. *Applied optics* 58.13 (2019): D68-D75.

Luminescence decay behavior in doped TBC configurations

Extension of Kubelka-Munk model - Results

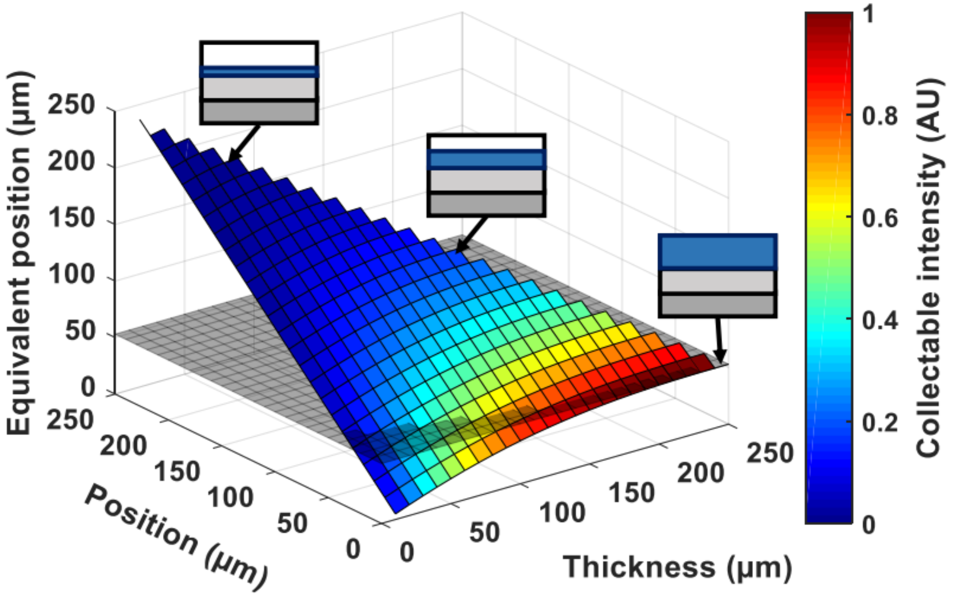

Results for YSZ:Er for 325 doped TBC configurations (resolution 10 μm)

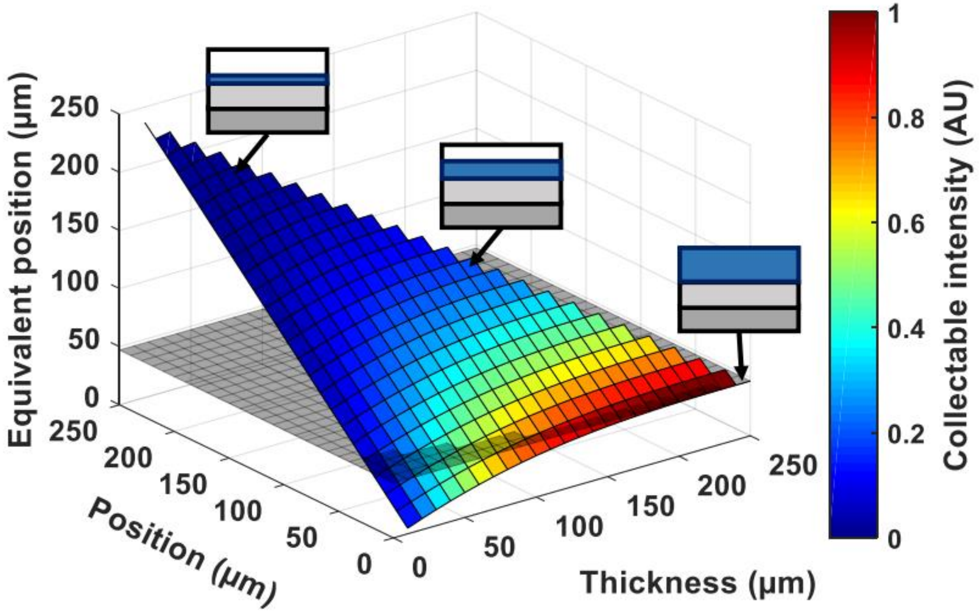

Results for YSZ:Sm for 325 doped TBC configurations (resolution 10 μm)

Fouliard, Q., et al. *Applied optics* 58.13 (2019): D68-D75.